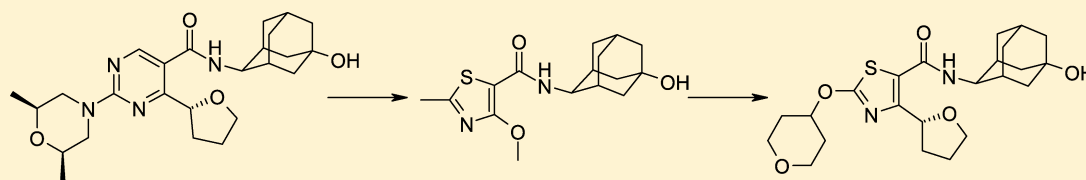


Optimization of Brain Penetrant 11 β -Hydroxysteroid Dehydrogenase Type I Inhibitors and in Vivo Testing in Diet-Induced Obese Mice

Frederick W. Goldberg,* Alexander G. Dossetter,* James S. Scott, Graeme R. Robb, Scott Boyd, Sam D. Groombridge, Paul D. Kemmitt, Tove Sjögren, Pablo Morentin Gutierrez, Joanne deSchoolmeester, John G. Swales, Andrew V. Turnbull, and Martin J. Wild

AstraZeneca, Mereside, Alderley Park, Macclesfield SK10 4TG, United Kingdom

Supporting Information



Compound	3	5	40
h-11 β -HSD1 HPLC	4.5 nM	28 nM	1.7 nM
Free rat [Brain] / [Blood]	0.3	1.2	1.1

ABSTRACT: 11 β -Hydroxysteroid dehydrogenase type 1 (11 β -HSD1) has been widely considered by the pharmaceutical industry as a target to treat metabolic syndrome in type II diabetics. We hypothesized that central nervous system (CNS) penetration might be required to see efficacy. Starting from a previously reported pyrimidine compound, we removed hydrogen-bond donors to yield **3**, which had modest CNS penetration. More significant progress was achieved by changing the core to give **40**, which combines good potency and CNS penetration. Compound **40** was dosed to diet-induced obese (DIO) mice and gave excellent target engagement in the liver and high free exposures of drug, both peripherally and in the CNS. However, no body weight reduction or effects on glucose or insulin were observed in this model. Similar data were obtained with a structurally diverse thiazole compound **51**. This work casts doubt on the hypothesis that localized tissue modulation of 11 β -HSD1 activity alleviates metabolic syndrome.

INTRODUCTION

11 β -Hydroxysteroid dehydrogenase type 1 (11 β -HSD1) is a NADPH-dependent enzyme that is widely expressed, notably in liver, adipose tissue, and brain.¹ It catalyzes conversion of the inactive glucocorticoid hormone cortisone to the active glucocorticoid hormone cortisol and therefore plays a key role in the regulation of intracellular cortisol concentrations.² Although patients with metabolic syndrome do not exhibit elevated plasma glucocorticoid levels,³ it has been hypothesized that elevated intracellular concentrations may play a crucial role, and reduction of these has been proposed as an attractive therapeutic paradigm.^{4–6} Elevated cortisol is also associated with cognitive dysfunction and neurotoxicity, and glucocorticoids increase amyloid A β in models of Alzheimer's disease (AD). 11 β -HSD1 is highly expressed in brain regions important for cognition and is increased in animal models of AD. Transgenic overexpression of 11 β -HSD1 in brain exacerbates age-associated cognitive dysfunction, while 11 β -HSD1 knock-out mice are protected.^{7,8} Proof of concept has been obtained in humans by use of the nonselective prototype 11 β -HSD inhibitor carbenoxolone.⁹

Over 250 11 β -HSD1 patent applications from more than 25 pharmaceutical companies and academic groups have now been

published, with the primary focus on treatment of metabolic syndrome.^{10,11} Incyte has taken an undisclosed compound as far as phase II trials in patients with type II diabetes.¹² Doses of 200 mg resulted in small reductions in glycated hemoglobin (hBA1c, -0.6%), fasting glucose (-24 mg/dL), and reduction in homeostatic model assessment-insulin resistance (HOMA-IR, -24%) compared with placebo. Merck has progressed two compounds into development: 3-[1-(4-chlorophenyl)-3-fluorocyclobutyl]-4,5-dicyclopropyl-1,2,4-triazole (MK-0916), which entered phase II in 2004, and 3-[1-(3-ethylsulfonylpropyl)-4-bicyclo[2.2.2]octanyl]-4-methyl-5-[2-(trifluoromethyl)phenyl]-1,2,4-triazole (MK-0736), which was originally developed as a treatment for hypertension and entered phase II trials in 2005.¹³ Initial clinical data have now been reported showing no significant improvement in fasting plasma glucose at week 12 relative to placebo. Modest dose-dependent decreases in blood pressure and body weight were observed over the course of the study, together with a small but significant reduction of 0.3% in hBA1c at week 12.¹⁴ Collectively these data indicate that only high doses of 11 β -

Received: October 28, 2013

Published: January 14, 2014

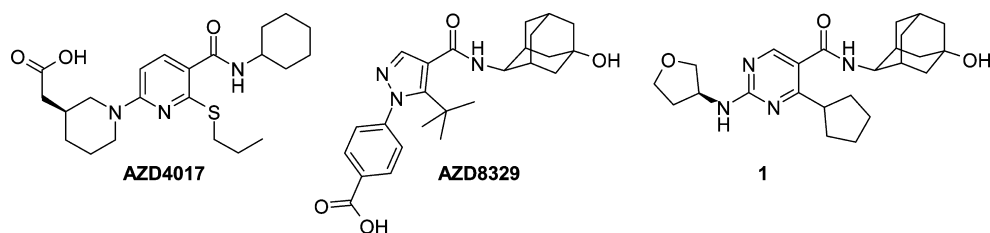
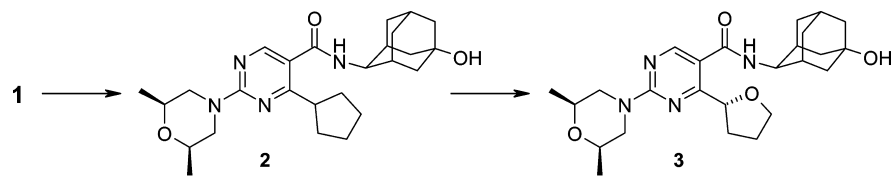


Figure 1. Structures of potential start points.



Compound	1	2	3
h-11β-HSD1 IC ₅₀ (nM) ^a	21 (19-24)	27 (25-29)	33 (27-40)
m-11β-HSD1 IC ₅₀ (nM) ^a	32 (28-36)	412 (371-458)	58 (49-68)
logD _{7.4}	2.4	3.6	2.3
MW / PSA	426 / 99	454 / 86	456 / 94
Rat F% ^b	64	70	35
MDCK P _{app} A-B (x10 ⁻⁶ cm/s)	3	20	23
MDCK Efflux Ratio	11	1.4	1.7

Figure 2. Optimization of pyrimidine-based 11β-HSD1 inhibitors for CNS properties. ^ah denotes human isoform; m denotes murine isoform. IC₅₀ data are the geometric mean of at least three independent measurements unless stated, with 68% confidence limits in parentheses as calculated from standard error of the mean (SEM). ^bDosed individually (HPMC/Tween suspension for po and solution for iv) to fed male Han Wistar rats.

HSD1 inhibitors improve glycemic control in humans and do so only to a modest extent.

Our own experience with 11β-HSD1 inhibitors in the preclinical setting¹⁵ mirrors the clinical work and indicates that only very high doses/exposures of 11β-HSD1 inhibitors provide efficacy. We hypothesized that modest central nervous system (CNS) penetration may account for the limited efficacy and high doses required. 11β-HSD1 is expressed in areas of the brain relevant to metabolic control,¹⁶ and glucocorticoids are known to have effects on neuropeptides in the hypothalamus, including proopiomelanocortin (POMC) and neuropeptide Y (NPY), which are crucially involved in food intake and have also been shown to control glucose levels via the vagal nerve.^{17,18}

RESULTS AND DISCUSSION

To explore the hypothesis that 11β-HSD1 inhibition in the brain (in addition to peripheral tissues) may cause effects on body weight or glycemic control, we required tool compounds with good CNS exposure. Acidic compounds such as 2-[(3S)-1-[5-(cyclohexylcarbamoyl)-6-propylsulfanyl-2-pyridyl]-3-piperidyl]acetic acid (AZD4017, Figure 1)¹⁹ and 4-[4-(2-adamantylcarbamoyl)-5-tert-butylpyrazol-1-yl]benzoic acid (AZD8329)²⁰ were considered unlikely to deliver a brain penetrant profile, so we instead chose neutral pyrimidines such as 1 as potential start points, as they are neutral compounds

with good pharmacokinetics (PK) and are potent against both human and murine isoforms.^{15,21}

Our initial strategy to improve CNS penetration was to reduce the number of hydrogen-bond donors present in 1 with a view to reducing the levels of efflux as measured by a Madin–Darby canine kidney (MDCK) assay.²² Replacement of the amino-tetrahydrofuran (THF) at C2 with a 3,5-*cis*-dimethyl-substituted morpholine 2 (Figure 2) retained human potency but was significantly less potent in mouse, in accordance with previous structure–activity relationships (SAR) on this series.¹⁵ The favorable DMPK properties in rat were retained despite a significant increase in log *D*_{7.4} (+1.2) associated with this change. To lower the lipophilicity, we investigated ether substitution into the 5-membered ring and found that the 2-(*R*)-tetrahydrofuryl²³ analogue 3 lowered log *D*_{7.4} (−1.3) while maintaining human potency and improving mouse potency to a level comparable to 1. This compound has two hydrogen-bond donors with one potentially “masked” through formation of a 7-membered internal hydrogen bond between the amide NH and the ether, whereas 1 has three hydrogen-bond donors. It is noteworthy that the ¹H NMR shift in CDCl₃ of the amide NH in 3 is shifted downfield ($\delta_{\text{H}} = 7.90$ ppm) relative to 2 ($\delta_{\text{H}} = 5.83$ ppm), consistent with formation of an internal hydrogen bond. MDCK permeability of 2 and 3 was notably improved relative to 1 with no significant efflux observed, presumably as a consequence of the reduced hydrogen-bond donor count.²⁴

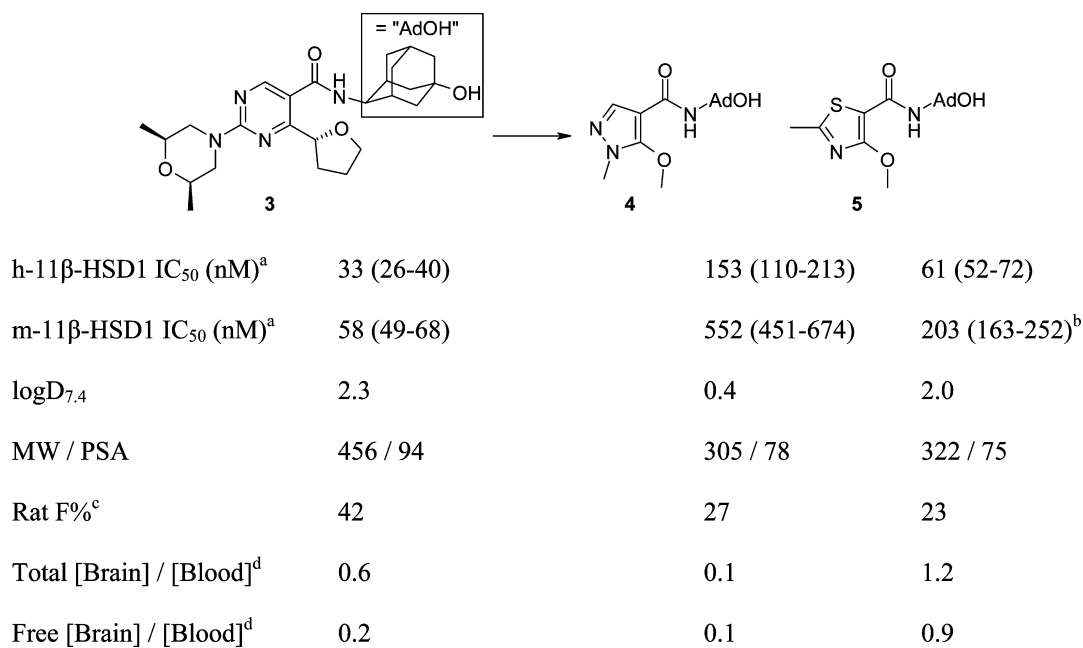


Figure 3. Changing the core to identify new CNS penetrant lead compounds. ^ah denotes human isoform; m denotes murine isoform. IC₅₀ data are the geometric mean of at least three independent measurements unless stated, with 68% confidence limits in parentheses as calculated from the SEM. ^b*n* = 2. ^cDosed individually (HPMC/Tween suspension for po and solution for iv) to fed male Han Wistar rats. ^dRatio of the mean (*n* = 2) drug concentrations in homogenized brain tissue and whole blood, 1 h after a 30 mg/kg dose to male Han Wistar rats.

Compound 3 achieved moderate CNS exposure (free ratio 0.24), although the molecular mass (456 Da) and polar surface area (PSA; 94 Å², not accounting for intramolecular hydrogen bond) were high compared to those of known neutral CNS-penetrant drugs.²⁵ Efforts to reduce donor count further by changing the 1-hydroxyadamantyl group were unsuccessful, as they led to significant reductions in potency and/or poor PK properties. We therefore attempted to identify a new core that might allow us to reduce molecular mass while maintaining good potency against both human and murine isoforms. We synthesized a range of core heterocycles, fixing the 1-hydroxyadamantyl from pyrimidine 3 and maintaining an ortho group to the amide (Figure 3), as our experience had shown that this was required for potency. A pragmatic high-throughput approach was taken to assess CNS penetration, where compounds with acceptable human and murine potency in a homogeneous time-resolved fluorescence (HTRF) assay and rat PK in cassette were assessed for CNS penetration individually, by orally dosing 30 mg/kg of compound to rats and assessing the brain/blood ratio at a fixed 1 h time point. Rat was chosen as the species to assess CNS penetration as blood contamination of brain samples can be an issue when CNS penetration is assessed in mouse. Free [brain]/[blood] ratios could then be determined by correcting the total ratio with *in vitro* tests for plasma protein binding and brain slice tissue binding. All rat PK measurements in this article are taken from whole blood (not plasma), as compounds from this series were observed to partition unequally between red blood cells and plasma.

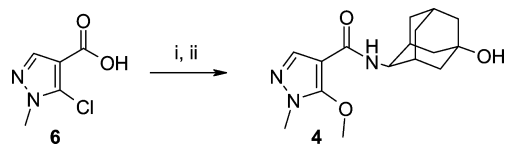
f

We started by synthesizing pyrazole 4 (Figure 3), given the precedent of this ring system from a previous acidic series²⁰ and the knowledge from our previous work that alkoxy substituents can achieve good human and murine potency.¹⁵ Compound 4 had good human/murine potency and suitable PK for assessment of CNS penetration, but the measured free

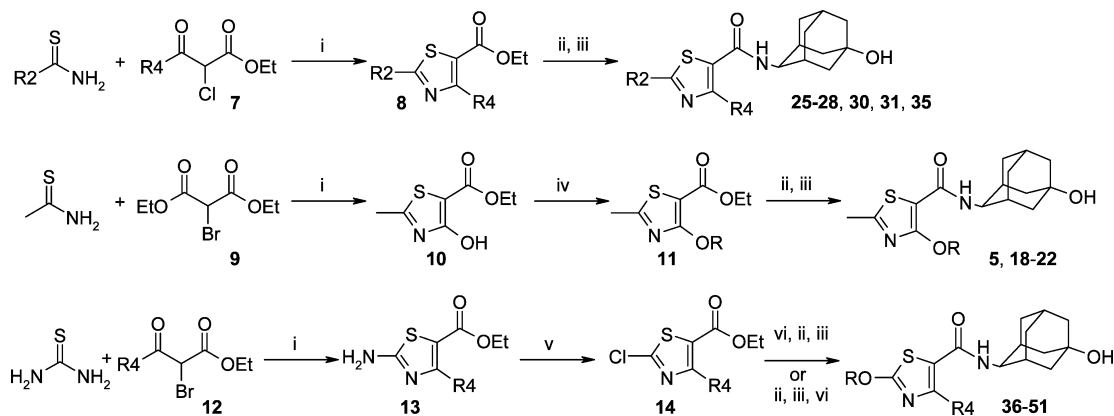
[brain]/[blood] ratio using the above method was poor (0.1), albeit at very low log *D*_{7.4} (0.4). Other pyrazoles we synthesized (with higher log *D*) gave poor oral exposure, so we investigated alternative heterocycles. This work identified only one compound, 5, that showed excellent CNS penetration (~1:1 free ratio at 1 h time point), with good potency against both human and murine isoforms despite its low molecular weight (322). Thiazole 5 was therefore selected as a suitable lead compound for further optimization. Thiazole 5 had good physicochemical properties (log *D*_{7.4} = 2.0, solubility >2 mM), high free levels (Hu ppb = 55% free, brain tissue binding = 40% free), and moderate oral bioavailability (23%) and clearance (22 mL·min⁻¹·kg⁻¹) in rat. Our priority was therefore to improve human/murine potency and oral exposure of 5 while maintaining the excellent physicochemical properties (maintain log *D*_{7.4} between 1 and 3).

Pyrimidines 1–3 were synthesized according to previously published procedures and general methods.^{15,21} Pyrazole 4 was synthesized by an amide coupling between (1*S*,4*R*)-4-aminoadamantan-1-ol and 2-chloropyrazole 6, followed by methoxide displacement of the chloride (Scheme 1). Thiazoles 5 and 15–51 were typically synthesized by a late-stage coupling of a thiazole acid with both R² and R⁴ groups in place, formed from saponification of the corresponding ester (Scheme 2). The route used to synthesize the ester precursor varied, depending

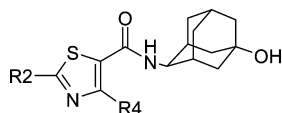
Scheme 1. Synthesis of Pyrazole 4^a



^aReagents and conditions: (i) (1*S*,4*R*)-4-Aminoadamantan-1-ol hydrochloride, HATU, DMF, *i*-PrNEt₂, 68%. (ii) NaOMe, THF, 54%.

Scheme 2. General Synthetic Routes to Vary R² and R⁴ Groups on the Thiazole^a

^aReagents and conditions: (i) Toluene or EtOH, 25–88%. (ii) NaOH, EtOH or KOSi(CH₃)₃, THF, 64–100%. (iii) (1*S*,4*R*)-4-Aminoadamantan-1-ol hydrochloride, HATU, DMF or CH₂Cl₂, *i*-PrNEt₃, 31–91%. (iv) DIAD, THF, PPh₃, ROH, THF or RI, K₂CO₃, DMF, 26–99%. (v) *t*-BuONO, THF, HCl, 1,4-dioxane, 68–78%. (vi) NaOR, ROH or THF, 48–85%

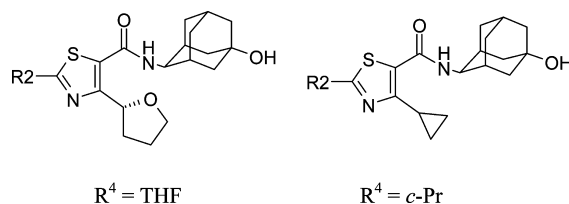
Table 1. Optimizing the R⁴ Group

5	R ²	R ⁴	IC ₅₀ ^a nM (68% CL)			LLE ^c	log D _{7.4}	aq solubility, ^d μM	[brain]/[blood] ^b		PSA, Å ²
			h-11β-HSD1, HTRF	m-11β-HSD1, HTRF	h-11β-HSD1, HPLC				total	free	
5	Me	OMe	61 (52–72)	203 (163–252) ^e	28 (26–30)	5.2	2.0	>2000	1.2	0.9	75
15	H	OMe	142 (126–160)	304 (266–347)		5.2	1.7	2100			75
16	H	H	>20500 ^e	>24400 ^e		<3.9	0.8	>2900			66
17	Me	Me	8600 (7110–10400)	6910 (4810–9920)		3.8	1.3	>1500			66
18	Me	OEt	29 (28–30)	179 (141–228)		4.9	2.6	170			75
19	Me	OCH ₂ CF ₃	23 (18–29)	637 (562–722)	8.3 (7.9–8.8)	4.5	3.1	210			75
20	Me	O- <i>i</i> -Pr	13 (11–15)	364 (344–386)		4.9	3.0	65			75
21	Me	O- <i>c</i> -Bu	10 (9–11)	125 (114–138)		4.8	3.2	64			75
22	Me	O-(3-oxetenyl)	104 (95–113)	4810 (3390–6820)		5.5	1.5	1100			84
23	Me	<i>S</i> - <i>n</i> -Pr	14 (11–18)	1040 (908–1200)		4.8	3.1	500			66
24	Me	CF ₃	2090 (1730–2530)	9350 (7870–11100)		4.2	1.5	610			66
25	Me	<i>c</i> -Pr	69 (65–74)	395 ^f		5.3	1.9	920	1.6	1.2	66
26	Me	(<i>S</i>)-2-THF	216 (193–242)	11600 (8430–16000)		4.9	1.8	>2100			74
27	Me	(<i>R</i>)-2-THF	24 (19–29)	364 (189–700)	3.6 (2.6–4.9)	5.8	1.8	>2100	1.5	2.9	74

^ah denotes human isoform; m denotes murine isoform. IC₅₀ data are the geometric mean of at least three independent measurements unless stated, with 68% confidence limits in parentheses as calculated from SEM. ^bRatio of mean (*n* = 2) drug concentrations in homogenized brain tissue and whole blood, 1 h after a 30 mg/kg dose to male Han Wistar rats. ^cLigand lipophilicity efficiency, defined as human HTRF pIC₅₀ – log D_{7.4}. ^dAqueous solubility measured at pH 7.4, performed under thermodynamic conditions from solid samples. ^e*n* = 2. ^f*n* = 1.

on the nature of the R² and R⁴ groups. Where R² and R⁴ were both alkyl groups, classic Hantzsch ring synthesis between a 2-

chloro ketoester 7 and a thioamide was used to give ester 8, which could then be saponified and coupled with (1*S*,4*R*)-4-

Table 2. Optimizing the R² Position, with R⁴ Fixed as either (R)-2-THF or Cyclopropyl

R ²	IC ₅₀ ^a nM (68% CL)			LLE ^c	log D _{7.4}	aq solubility, ^d μM	rat F (%) / rat CL (mL·min ⁻¹ ·kg ⁻¹) ^e	[brain] / [blood] ^b total/free	PSA, Å ²
	h-11β-HSD1, HTRF	m-11β-HSD1, HTRF	h-11β-HSD1, HPLC						
R⁴ = THF									
27 Me	24 (19–29)	364 (189–700)	3.6 (2.6–4.9)	5.8	1.8	>2100	11/17	1.5/2.9	74
28 Et	43 (36–51)	668 (604–738)		5.0	2.4	1600			74
29 H	10 (8–13)	360 (329–393)		6.4	1.6	>2600	0/52		74
30 CH ₂ OMe	48 (34–66)	3260 (2820–3760)		5.4	1.9	>7500			83
31 CH ₂ CH ₂ OMe	50 (40–62)	553 (493–621)		5.5	1.8				83
32 NH ₂	47 (36–61)	964 (878–1060)		5.6	1.7	710			102
33 NHMe	45 (36–56)	1210 (1060–1370)		5.3	2.1	560			89
34 NMe ₂	230 (206–255)	3980 (2690–5880)		3.9	2.7	140			75
35 CH ₂ SO ₂ Me	486 (358–658)	2480 (1920–3210)		5.9	0.4	1300	65/17	<0.05/<0.05	111
36 OMe	7.2 (6.5–8.0)	34 (30–37)	0.40 (0.30–0.53) ^f	5.8	2.3	490	40/21	1.1/0.7	84
37 OCH ₂ CH ₂ OMe	12 (10–15)	9.9 (9.7–10.1)	0.49 (0.40–0.60) ^f	5.8	2.1	980	24/8	0.8/1.0	92
38 (S)-OCH(Me) CH ₂ OMe	13 (11–15)	8.9 (6.5–12.2)	0.45 (0.40–0.50) ^f	5.1	2.8		16/13	0.9/0.5	92
39 O-(3-CN)- <i>c</i> -butyl	7.2 (6.7–7.6)	11.8 (8.9–15.6)		5.7	2.4	120			102
40 O-4-THP	17 (13–24)	14 (10–19)	1.7 (0.7–4.0) ^f	5.2	2.6	300	83/34	1.1/0.9	92
R⁴ = c-Pr									
25 Me	69 (65–74)	390 ^g		5.3	1.9	920	12/14	1.6/1.2	66
41 OMe	14 (12–16)	53 (49–57)	4.4 (4.398–4.44) ^f	5.3	2.6	570	45/15	1.8/0.7	75
42 OEt	9.1 (8.6–9.6)	34 (30–39)	1.7 (1.5–2.0) ^f	5.2	2.9	140			75
43 O- <i>i</i> -Pr	10 (9–12)	12 (11–13)	1.5 (1.1–2.0)	4.6	3.4	33			75
44 OCH ₂ CH ₂ OH	9.9 (8.9–11.0)	13 (11–16)		6.4	1.6	200	25/5	0.2/0.1	97
45 OCH ₂ CH ₂ OMe	17 (16–19)	23 (21–26)	2.8 (2.7–3.0) ^f	5.6	2.2	750	23/27	1.2/0.6	84
46 (R)-OCH(Me) CH ₂ OCH ₃	30 (27–33)	14 (11–18)	9.0 (5.5–14.8)	4.9	2.6	2700			84
47 (S)-OCH(Me) CH ₂ OMe	12 (11–14)	8.8 (7.0–11.0)	1.3 (0.9–2.0) ^f	5.1	2.8	960			84
48 O-(R)-2-THF	12 (11–14)	19 (16–23)	1.4 (1.0–2.0) ^f	5.5	2.4	260			84
49 O-4-THP	18	4.8	6.9	5.0	2.7	180	53/21	1.2/0.6	84

Table 2. continued

R ²	IC ₅₀ ^a nM (68% CL)			LLE ^c	log D _{7.4}	aq solubility, ^d μM	rat F (%) / rat CL (mL·min ⁻¹ ·kg ⁻¹) ^e	$\frac{[\text{brain}]}{[\text{blood}]}$ ^b total/free	PSA, Å ²
	h-11β-HSD1, HTRF	m-11β-HSD1, HTRF	h-11β-HSD1, HPLC						
R ⁴ = <i>c</i> -Pr	(15–22)	(4.1–5.7)	(5.1–9.5) ^f						
50 OCH ₂ - <i>c</i> -Pr	9.1 (8.3–9.9)	5.4 (4.7–6.1)	0.43 (0.40–0.46)	4.4	3.6	10			75
51 OCH ₂ -(1-CN)- <i>c</i> -Pr	22 (19–25)	13 (8–21)	8.1 (4.0–16.5) ^f	5.1	2.6	12	79/16	0.4/0.4	93

^ah denotes human isoform; m denotes murine isoform. IC₅₀ data are the geometric mean of at least three independent measurements unless stated, with 68% confidence limits in parentheses as calculated from SEM. ^bRatio of mean (*n* = 2) drug concentrations in homogenized brain tissue and whole blood, 1 h after a 30 mg/kg dose to male Han Wistar rats. ^cLigand lipophilicity efficiency, defined as human HTRF pIC₅₀ – log D_{7.4}. ^dAqueous solubility measured at pH 7.4, performed under thermodynamic conditions from solid samples. ^eCL = clearance; dosed individually (HPMC/Tween suspension for po and solution for iv) to fed male Han Wistar rats. ^f*n* = 2. ^g*n* = 1.

aminoadamantan-1-ol to give the target compounds. Where R⁴ = alkoxy, thioacetamide was condensed with diethyl 2-bromopropanedioate **9** to give **10**, which was then converted to alkoxy thiazole **11** via alkylation or Mitsunobu chemistry, and then converted to the final compounds as before. An exception to this route was **15**, where the R⁴ = OMe group was installed by displacement of a chloro with methoxy (see Supporting Information). The corresponding thioethers at R⁴ were generated from alkylation of a thiol as detailed in Supporting Information for **23**. To synthesize examples with R² = alkoxy, we first condensed thiourea with bromo ketoester **12** to generate 2-aminothiazole **13**, followed by conversion to the corresponding 2-chlorothiazole **14**. Compound **14** could be converted through to the final compounds by displacing the chloro with an alkoxide, followed by saponification of the ester and amide coupling. Alternatively the ester of **14** could be saponified first, followed by amide coupling and displacement of the chloro as the last step. 2-Aminothiazole **12** could also be functionalized directly when alkylamine R² groups were desired in the final compound, as detailed in Supporting Information for **33** and **34**.

These synthetic routes allowed us to vary the R² and R⁴ groups on the thiazole and assess the SAR. Simple thiazole amides **15** and **16** (Table 1) suggested that removal of the methyl at R² was tolerated but that a group at R⁴ was required for potency. Compound **17** demonstrated that a methyl group at R⁴ was much less potent than methoxy. Larger lipophilic alkoxide groups at R⁴ (**18–21**) increased potency, although LLE (ligand lipophilicity efficiency, pIC₅₀ – log *D*) was not improved. A more polar 3-oxetanyl group **22** was well tolerated for human potency, considering the low log *D* and favorable physical properties, but gave poor mouse potency. Sulfur-linked alkyl chains were also explored to give **23**, given the precedent from a previous program.¹⁹ This gave excellent potency against the human isoform but poor potency against the murine isoform and very poor stability in rat hepatocytes, so this approach was not pursued further. The murine potency result for **23** was in line with our expectation from the published crystal structures that the murine isoform does not tolerate very large groups at R⁴. We also explored alkyl R⁴ groups, where larger groups such as cyclopropyl **25** and (*S*)-2-THF **27** gave comparable HTRF potency, metabolic stability, and solubility to the methoxy start point **5**. The *S*-THF enantiomer **26** was 10 times less potent than the *R* enantiomer, as expected from our experience with pyrimidines, where the *R* stereochemistry in **3** was also the more potent enantiomer. To further profile **5**, **25**,

and **27** as start points for optimization, we checked whether the favorable [brain]/[blood] ratio had been maintained, and we also assessed potency of **5** and **27** in a low-throughput HPLC 11β-HSD1 assay. The HPLC assay was better at accurately assessing the potency of very potent compounds that approach the tight binding limit of the HTRF assay, as the greater sensitivity of the HPLC assay meant that we could lower the enzyme concentration 10-fold, so very potent compounds appeared more potent in the HPLC assay. The THF compound **27** was more potent in the HPLC assay than **5**, and both **25** and **27** maintained high [brain]/[blood] ratios, consistent with the low PSA (all compounds in Table 1 have calculated PSA < 80 Å²). Note the unusually high ratio of 2.9 for **27** is due primarily to the measured differences in brain tissue versus plasma protein binding for that compound; the total [brain]/[blood] ratio was 1.5. We felt that alkyl R⁴ groups such as THF and cyclopropyl offered broader scope for further optimization than alkoxy groups, as they allow us to vary R² more widely, as for example, if R² and R⁴ are both alkoxy, the resulting thiazoles were found to be unstable.

We then assessed the SAR of the R² position (Table 2), focusing primarily on compounds with R⁴ = THF, although we also synthesized some examples with R⁴ = *c*-Pr. Removing the methyl to give **29** was tolerated, and in fact the resulting compound has excellent LLE (6.4) as a consequence. However, as **29** gave modest murine potency and poor rat PK, we subsequently focused on compounds with R² substituents. Ethyl **28** was of similar potency to methyl **27** against both isoforms, with worse LLE (5.0). However, **28** did allow us to generate our first high-resolution crystal structure from this series (a structure had been obtained previously with **5** but at low resolution). The crystal structure for **28** (4c7k, resolution 1.9 Å, Figure 4) shows the expected pair of hydrogen bonds from the ligand carbonyl to Ser170 and Tyr183, and the adamantyl hydroxy group takes part in an extended hydrogen-bonding network with several crystallographic waters and the NADP(H) cofactor. When comparing this structure to the previously obtained structure of pyrimidine **1** (4bb5), we observed the loss of a weak hydrogen bond to Gly216 due to the absence of the corresponding hydrogen-bond acceptor in the thiazole ring. However, this is compensated by an additional interaction between Leu215 and the sulfur atom of the thiazole, the result of electron density transfer from the electron-rich carbonyl to the electron-deficient sulfur. The strength of this interaction is expected to be similar in magnitude to a typical hydrogen bond.²⁶ The dihedral angle between the aromatic ring

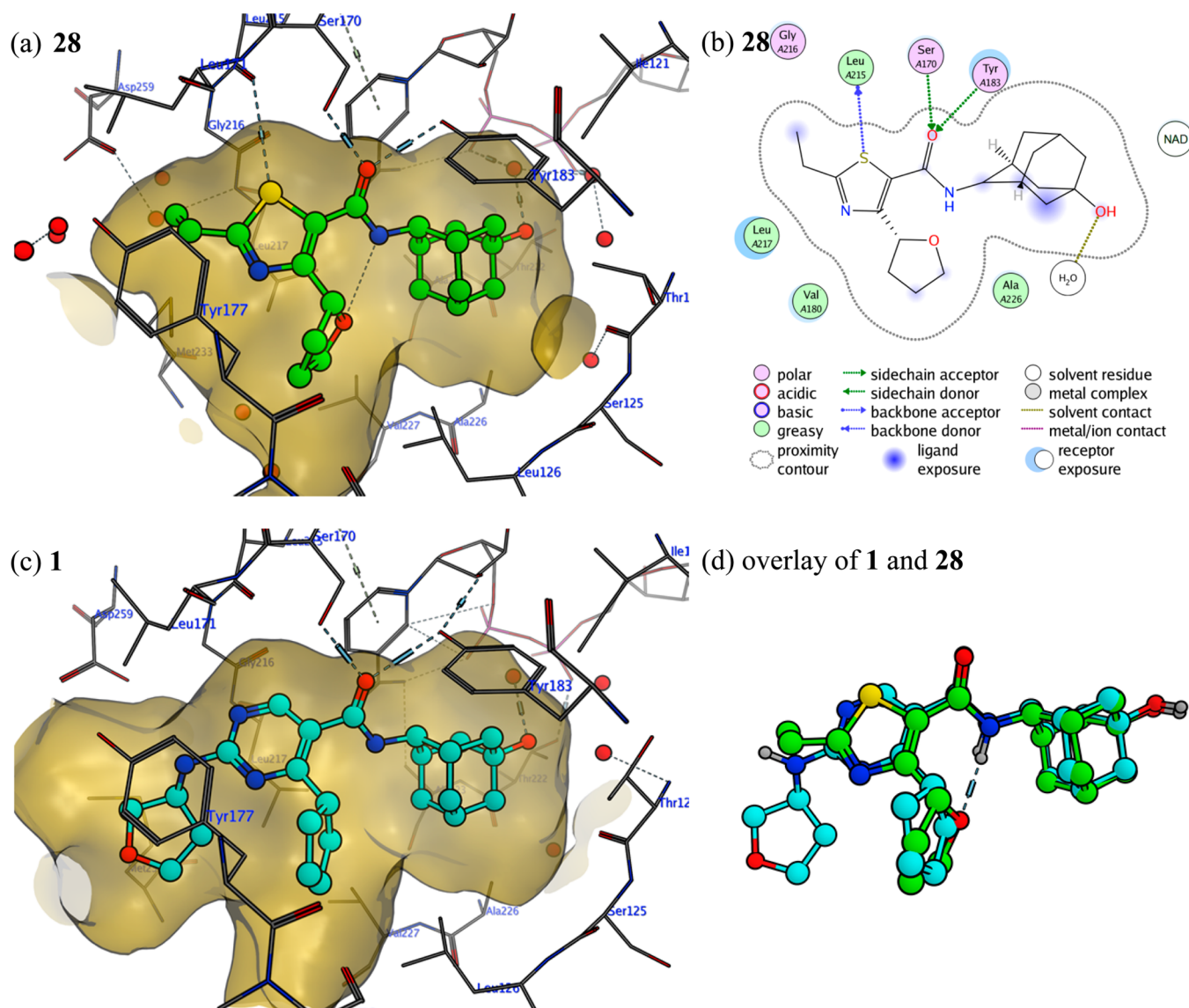


Figure 4. Selected ligands cocrystallized with human isoform of 11 β -HSD1: (a) ligand binding pocket of **28** (4c7k); (b) interaction map showing directional interactions; (c) ligand binding pocket of **1** (4bb5); (d) overlay of **28** (green carbons) and **1** (cyan carbons).

and the amide is approximately the same between pyrimidine **1** and thiazole **28** (56° for pyrimidine, 41° for thiazole; note the presence of an intramolecular hydrogen bond for the thiazole that is not present in the pyrimidine). This positions the R^4 group of both ligands into the same lipophilic pocket, with the potential for larger groups to be tolerated. The orientation of the R^2 group of the thiazole differs somewhat from the equivalent group in the pyrimidine ligand and so we would not expect substituent SAR to transfer directly from one series to the other.

By maintaining $R^4 = \text{THF}$, we were able to explore a wide diversity of R^2 groups; in particular, we aimed to place polar groups in the R^2 region, as we expected from the crystal structure that these may be tolerated. Changing methyl to methoxymethyl (**30**, Table 2) maintained human potency but reduced murine potency. However, spacing the methoxy out with an additional methylene to give **31** restored the murine potency, which demonstrated that correct placement of polarity could maintain potency against both isoforms. SAR remained flat with NH_2 and NHMe groups (**32** and **33**), but NMe_2 **34**

was less active. A side chain bearing a sulfone group **35**, designed with the intention of making a polar interaction, was significantly less active, although LLE is maintained due to a low $\log D$ (0.4). As well as giving a lower $\log D$ than we typically explored, **35** gives a high calculated PSA (111 \AA^2), and interestingly we observed poor CNS exposure for **35** (total ratio 0.03), despite having high bioavailability in rat (65%).

Switching to O-linked R^2 groups gave us a breakthrough: methoxy **36** had excellent potency against both isoforms, close to the tight binding limit of the human assay, so potency was assessed in the HPLC assay as being 0.4 nM. Further alkoxy examples **37–40** all proved to be very potent against both isoforms, and **37**, **38**, and **40** were bioavailable in rat and had excellent CNS penetration (free ratio $\sim 1:1$ at 1 h time point). The alkoxy groups in **37–40** were selected for synthesis on the basis of the more extensive set made with $R^4 = c\text{-Pr}$ (vide infra). These compounds were further profiled in mouse, and **40** was taken forward as a key probe compound to explore preclinical efficacy.

With the data in hand on the significant benefit of $R^2 =$ alkoxy, we also explored compounds with other alkyl groups in the R^4 position, in particular $R^4 = c\text{-Pr}$. As shown in Table 2, the SAR with $R^4 = c\text{-Pr}$ is broadly similar to that obtained with $R^4 =$ THF. Methoxy **41** was again found to be more potent than methyl **25**, particularly against the murine isoform. This result led to the synthesis of a range of alkoxy groups **42–51**, which generated several very potent compounds with suitable PK properties to be considered as probe compounds. The crystal structure of **28** was used to inform the design of these compounds, notably **44** (pendant alcohol), which was designed to displace an observed crystallographic water and thus gain additional potency and improved LLE. Figure 5 shows the

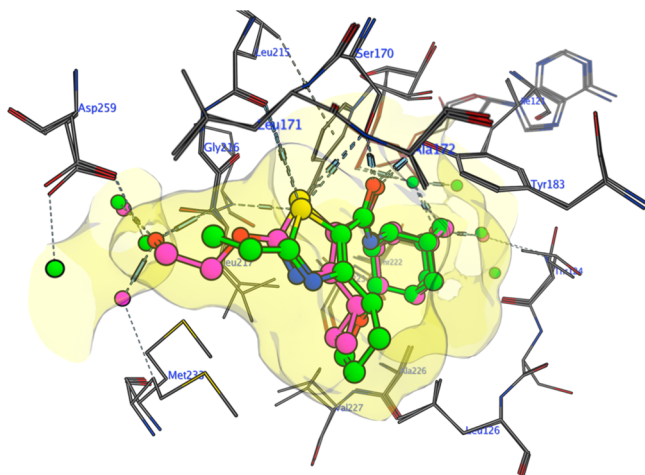


Figure 5. Overlay of **28** ($R^4 =$ ethyl, ligand carbons and solvent atoms in green, 4c7k) and **44** ($R^4 =$ $\text{OCH}_2\text{CH}_2\text{OH}$, ligand carbons and solvent atoms in magenta, 4c7j). The hydroxyl group of **44** displaces a crystallographic water present in the crystal structure of **28**.

overlay of the crystal structures of **28** and **44** (4c7j, resolution 2.2 Å), with the side chain of **44** displacing the water molecule as intended. This is further reflected in the measured potency, with potency maintained with respect to ethoxy **42** at reduced $\log D$ ($\Delta \log D = -1.3$), and consequently **44** has excellent LLE (6.4). However, although CNS penetration for the $R^4 = c\text{-Pr}$ examples was generally good, **44** is an exception. It is interesting to contrast **44** (hydroxy, free ratio 0.1) with the close analogue **45** (methoxy, free ratio 0.6), where once again it appears that high PSA, or more specifically hydrogen-bond

donor count in this case, appears to reduce the free [brain]/[blood] ratio.

In general, it can be seen that the compounds with $R^4 =$ THF are more potent than the corresponding matched pairs with $R^4 = c\text{-Pr}$, and **40** in particular was considered a suitable probe compound for further studies. However, as we were keen to take two structurally diverse compounds into efficacy studies, we profiled both **40** and **51** in mouse PK, where they both showed good oral exposure (Table 3). Both compounds were tested for $11\beta\text{-HSD2}$ inhibition and were found to be inactive, which is important as $11\beta\text{-HSD2}$ is believed to be responsible for the reverse reaction in vivo ($11\beta\text{-HSD1}$ converts cortisone to cortisol, whereas $11\beta\text{-HSD2}$ converts cortisol to cortisone), and $11\beta\text{-HSD2}$ activity has been associated with increased risk of hypertension.²⁷

Before proceeding to efficacy studies in mice, we examined whether these compounds could deliver target engagement in the brain and established a pharmacokinetic/pharmacodynamic (PK/PD) relationship, which due to technical issues was done in the rat. Compound **51** was selected for this study as it had good potency against the rat isoform with HTRF $\text{IC}_{50} = 55$ nM (68% confidence limit from SEM 42–70 nM), whereas **51** had modest rat potency of 345 nM (265–449 nM). A dose response study was designed with rats receiving a single oral dose of **51**. One hour postdose (to coincide with C_{max} in plasma) the animals were terminated, compound concentrations in plasma and brain were quantified, and target engagement in CNS was assessed by comparing the ratio of corticosterone/dehydrocorticosterone (DHC) between the groups. Figure 6 shows the PK/PD relationship between corticosterone/DHC ratio and drug concentrations, in both plasma and CNS. The resulting PK/PD fit suggests that the in vivo IC_{50} (49 nM vs plasma PK, 20 nM vs brain PK) corresponds closely to the in vitro IC_{50} (55 nM by HTRF) within error. It should be noted that there is considerable variability in the PD data as evident from the plots in Figure 6, giving a ± 2 -fold variability in the estimated IC_{50} . This study gave us confidence that where the free compound concentration exceeded the in vitro IC_{50} , we should obtain target engagement in vivo, both peripherally and in the brain. More specifically, where free compound concentration $>10\times \text{IC}_{50}$, then total target engagement should be obtained. A reduction of the activity of $11\beta\text{-HSD1}$ in the CNS was also observed in this study by means of an ex vivo assay (conversion of ^3H -cortisone to ^3H -cortisol).

Table 3. Pharmacokinetic Data for **40** and **51**

species	PPB % free	hep $\text{CL}_{\text{intv}}^a$ $\mu\text{L}\cdot\text{min}^{-1}\cdot 10^{-6}$	iv/po dose, ^b $\mu\text{mol}\cdot\text{kg}^{-1}$	iv $\text{CL},^b$ $\text{mL}\cdot\text{min}^{-1}\cdot\text{kg}^{-1}$	iv $V_{\text{ss}},^b$ $\text{L}\cdot\text{kg}^{-1}$	po AUC, ^b $\mu\text{M}\cdot\text{h}$	F, %
Compound 40							
rat ^c	20	12	5.2/7.4	34	1.0	3.9	83
mouse ^d	22	11	3.5/17.6	26	1.7	20.6	139
human	23	<3					
Compound 51							
rat ^c	20	22	3.1/12.3	16	0.6	7.9	79
mouse ^d	22	25	4.0/14.3	18	1.0	12.0	73
human	16	<3					

^aIn vitro median intrinsic clearance observed with hepatocytes from the appropriate species. ^bAll measurements were taken from whole blood (not plasma), as compounds from this series were observed to partition unequally. iv, intravenous; po, per os; CL, clearance; V_{ss} , steady-state volume of distribution; AUC, area under curve. ^cDosed individually (HPMC/Tween suspension for po and solution for iv) to fed male Han Wistar rats. ^dDosed individually (HPMC/Tween suspension for po and solution for iv) to fed male C57B6 mice.

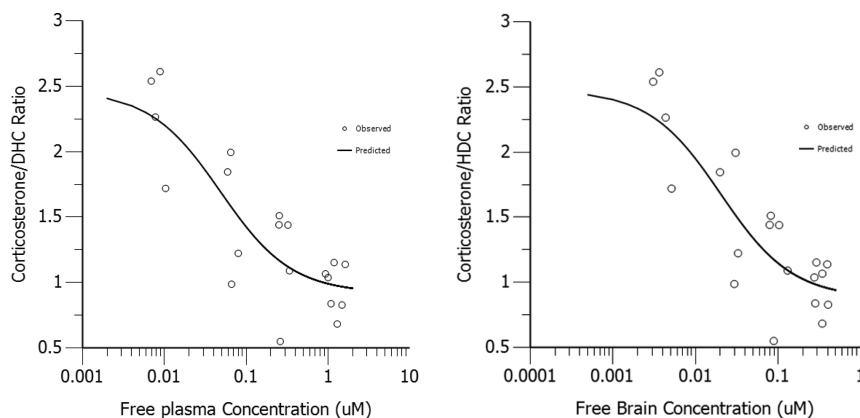


Figure 6. PK/PD relationship of **51** in the rat, comparing PD activity in the brain versus PK in plasma (left, $IC_{50} = 49$ nM) or PK in brain (right, $IC_{50} = 20$ nM). Points shown represent individual animals. More detailed parameters for model fitting can be found in Supporting Information (Table S2).

Compounds **40** and **51** were then evaluated for efficacy in a 21-day compound-in-diet (CID) study in C57B6 mice. Following similar protocols in the literature,²⁸ the mice in this study were fed a daily diet of 60% high-fat chow. The compound was finely ground and mixed with food and the mice, preconditioned on 60% high-fat diet, were allowed to eat 2.5 g/day. The CID protocol was devised to eliminate stress to the mice and avoid the possibility of adverse readings driven by elevated cortisol. In a scoping study for 5 days, all of the animals ate the required amount of food each day, which eliminated the possibility of any taste aversion stopping the animal receiving the correct calorie intake. Both compounds provided sufficient drug concentrations in the mouse CNS to test the 11β -HSD1 CNS hypothesis. Compound **51** gave a modest CNS ratio (free [brain]/[blood] ratio = 0.2) but still provided a free drug concentration in the brain of $20\times IC_{50}$ (HPLC) at 20 mg/kg. Compound **40** gave better CNS exposure (free [brain]/[blood] = 0.5–0.7) and gave free drug concentrations of $20\times IC_{50}$ (HPLC) at 4 mg/kg and $200\times IC_{50}$ (HPLC) at 40 mg/kg. Target engagement in the liver was confirmed by use of an ex vivo protocol, with both compounds showing high inhibition of 11β -HSD1 in the liver as shown in Figure 7. We could not directly assess CNS target engagement in mouse. However, as we achieved 20–200 $\times IC_{50}$ free drug concentration in the CNS and have both evidence of target engagement in the liver and confidence in our predictions from the PK/PD relationships in both plasma and brain in the rat, we were confident that we had achieved CNS target engagement in the efficacy study. Target engagement in adipose tissue could also not be directly shown in mouse. However, we have data from rats demonstrating that complete target engagement is observed when the free exposure exceeds the HPLC IC_{50} by >10-fold. As target engagement has been shown in the liver in the efficacy study in all study groups, and high peripheral IC_{50} cover has been achieved in the efficacy study (>10 \times HPLC IC_{50} in all study groups; for example, 280 \times HPLC IC_{50} for **40** at 40 mg/kg), we conclude that target engagement in adipose tissue was also achieved in this study.

No decrease in body weight or changes in insulin or glucose levels (and therefore HOMA-IR) in any of the animal groups were observed in the efficacy study, compared to the high-fat diet control (Figure 8). These data cast doubt on the hypothesis that localized tissue modulation of 11β -HSD1 activity, either peripheral or central, would alleviate metabolic

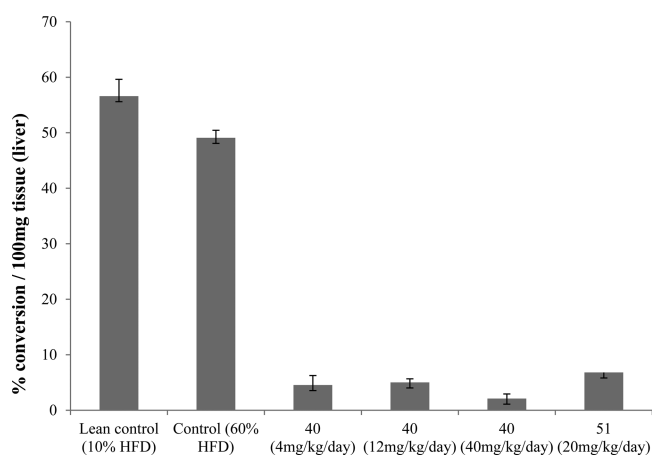


Figure 7. Ex vivo target engagement of **40** and **51** in liver in a mouse diet-induced obesity (DIO) efficacy study. Compound treated arms (for **40** and **51**) are in combination with 60% high-fat diet (HFD). Error bars denote 68% confidence limits as calculated from SEM ($n = 6$ for lean control, $n = 12$ for HFD control, $n = 10$ for each treated group).

syndrome. It should be noted that these data are consistent with the findings from recently published knockout data.²⁹ We noted that 11β -HSD1 programs in the literature had experienced activation of the pregnane X receptor (PXR)^{30–32} and inhibition of soluble epoxide hydrolase (sEH)^{33–35} and also general concerns that the positive preclinical efficacy of other 11β -HSD1 inhibitors may be due to off-target activities;¹³ therefore, we assessed our compounds for PXR activation and sEH inhibition. All 11 compounds tested (including **51**, but **40** was not assessed) were found to give <20% activation of PXR at 10 μ M. When assessed for sEH inhibition, **40** was found to be inactive ($IC_{50} > 33$ μ M), although **51** showed modest inhibition with IC_{50} of 12 μ M (68% confidence limit 7–20 μ M). Interestingly, pyrimidine **1** is a potent inhibitor of sEH with an IC_{50} of 22 nM (18–27 nM) and has previously demonstrated glucose and body weight efficacy at high doses.¹⁵ Compound **1** did not provide glucose efficacy at lower doses, despite providing target engagement of 11β -HSD1, and this study casts doubt on the hypothesis that this was due to it having poor CNS penetration. We conclude that it is possible that the positive efficacy observed at higher doses with **1** may have been due to sEH inhibition and/or

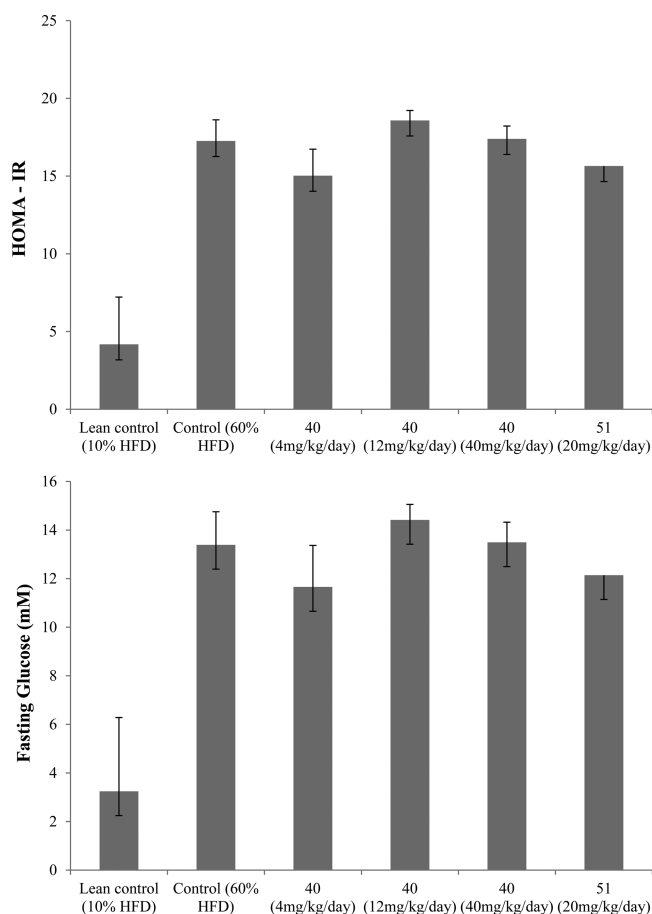


Figure 8. Effect on insulin resistance and fasting glucose of **40** and **51** in a mouse diet-induced obesity (DIO) 21-day study, showing no significant efficacy. HOMA-IR is defined as [fasting glucose (millimolar) \times fasting insulin (milliunits per liter)]/22.5. Error bars denote 68% confidence limits as calculated from SEM ($n = 6$ for lean control, $n = 12$ for HFD control, $n = 10$ for treated groups).

another unknown off-target mechanism, rather than due to 11β -HSD1 inhibition.

CONCLUSION

Starting from **3**, with low CNS penetration, we synthesized compounds with diverse heterocyclic cores and identified thiazole **5**, which had good potency, CNS penetration, and high LLE. We successfully optimized R^2 and R^4 positions on the thiazole and found that an oxygen atom at either position (but especially at R^2) increased potency. An oxygen linking atom at R^2 and a lipophilic group at R^4 were key for maximum inhibition. Compounds **40** and **51** were selected for efficacy studies on the basis of good murine potency, oral exposure, and CNS penetration. Both compounds were dosed to DIO mice by a CID protocol over 21 days. Excellent target engagement was achieved in liver, as assessed by an ex vivo assay, and by comparing the PK/PD relationship in rat to the high PK exposures in mouse in the efficacy study, we conclude that target engagement was also achieved in brain and adipose tissue. However, no body weight reduction or effects on glucose or insulin (and so HOMA-IR) were observed. This study does not support the hypothesis that 11β -HSD1 inhibition, either peripheral or central, markedly impacts body weight or glucose homeostasis. Whether 11β -HSD1 inhibitors have potential utility in other indications of either metabolic (e.g.,

atherosclerosis), cognitive (e.g., Alzheimer's disease), or inflammatory nature remains to be determined.

EXPERIMENTAL SECTION

General. All solvents and chemical used were reagent-grade. Purity and characterization of compounds were established by a combination of LCMS and NMR. LCMS spectra were obtained by use of a Waters liquid chromatography mass spectrometry system, where purity was determined by UV absorption at a wavelength of 254 nm and the mass ion was determined by electrospray ionization (Micromass instrument). All test compounds were >95% purity as assessed by LCMS and ^1H NMR. ^1H NMR spectra were recorded on a Varian AV400 FT spectrometer or via flow NMR process on an Avance 500 FT spectrometer, in deuterated dimethyl sulfoxide ($\text{DMSO}-d_6$) or CDCl_3 , with the data expressed as chemical shifts in parts per million (ppm) from internal standard tetramethylsilane (TMS). Preparative HPLC was performed on a Waters or Phenomenex column with decreasingly polar mixtures of water (containing 1% formic acid or 1% aqueous NH_4OH) and MeCN. Purification by flash column chromatography (FCC) was typically performed on silica gel (Merck 7734 grade), and solvent mixtures and gradients are recorded herein. All reactions were performed under nitrogen unless otherwise stated. All IC_{50} data are quoted as geometric means, and the 68% confidence intervals shown in parentheses are calculated from the SEM.

Synthesis of Representative Key Examples (3, 5, 27, 36, 40, and 51). *(2R)-Tetrahydrofuran-2-carbonyl Chloride.* N,N -Dimethylformamide (DMF; 0.015 mL, 0.20 mmol) was added to *(2R)*-tetrahydrofuran-2-carboxylic acid (2.3 g, 19.8 mmol) and oxalyl chloride (3.64 mL, 41.6 mmol) in dichloromethane (DCM; 25 mL) at room temperature (rt). The reaction mixture was stirred at rt for 20 h and then evaporated to afford the title compound (2.60 g, 98%), which was used without further purification. ^1H NMR (400 MHz, CDCl_3) 1.93–2.04 (2H, m), 2.19–2.28 (1H, m), 2.33–2.42 (1H, m), 3.99–4.07 (2H, m), 4.71–4.74 (1H, m), CO_2H not observed. LCMS not observed.

2,2-Dimethyl-5-[(2R)-tetrahydrofuran-2-carbonyl]-1,3-dioxane-4,6-dione. *(2R)*-Tetrahydrofuran-2-carbonyl chloride (2.6 g, 19.3 mmol) in DCM (5 mL) was added dropwise to 2,2-dimethyl-1,3-dioxane-4,6-dione (3.06 g, 21.3 mmol) and pyridine (3.13 mL, 38.6 mmol) in DCM (25 mL) at 0 °C. The reaction mixture was stirred at 0 °C for 1 h and at rt for 2 h and then was evaporated, diluted with DCM, and washed sequentially with 1 M aqueous citric acid, water, and saturated brine. The organic layer was dried over MgSO_4 , filtered, and evaporated to afford the title compound (4.28 g, 91%) as a brown oil that was used in the next stage without further purification. ^1H NMR (400 MHz, CDCl_3) 1.74 (6H, s), 1.86–1.94 (1H, m), 1.98–2.05 (2H, m), 2.57–2.68 (1H, m), 4.01–4.15 (2H, m), 5.65–5.70 (1H, m), 15.42 (1H, s). m/z $[\text{M} - \text{H}]^- = 241$. HPLC $t_R = 0.43$ min.

Methyl 3-Oxo-3-[(2R)-tetrahydrofuran-2-yl]propanoate. Methanol (25 mL) was added to 2,2-dimethyl-5-[(2R)-tetrahydrofuran-2-carbonyl]-1,3-dioxane-4,6-dione (4.28 g, 17.7 mmol) in toluene (50 mL) at rt. The reaction mixture was heated at reflux for 4 h and then allowed to cool to rt, evaporated, and purified by FCC, elution gradient 5–20% EtOAc in isohexane, to afford the title compound (1.80 g, 59%) as a colorless oil. ^1H NMR (400 MHz, CDCl_3) 1.85–1.95 (2H, m), 2.00–2.09 (1H, m), 2.15–2.24 (1H, m), 3.58 (2H, s), 3.74 (3H, s), 3.88–3.93 (2H, m), 4.36–4.39 (1H, m). m/z $\text{MH}^+ = 173$. HPLC $t_R = 0.80$ min.

Methyl (Z)-3-(Dimethylamino)-2-[(2R)-tetrahydrofuran-2-carbonyl]prop-2-enoate. DMF dimethyl acetal (1.67 mL, 12.6 mmol) was added in one portion to methyl 3-oxo-3-[(2R)-tetrahydrofuran-2-yl]propanoate (1.8 g, 10.5 mmol) in 1,4-dioxane (25 mL) at rt. The resulting solution was stirred at 100 °C for 2 h. The reaction mixture was evaporated, and the resulting crude product was purified by FCC, elution gradient 50–100% EtOAc in isohexane, to afford the title compound (1.80 g, 76%) as a yellow oil. ^1H NMR (400 MHz, CDCl_3) 1.83–1.92 (2H, m), 2.00–2.08 (1H, m), 2.12–2.21 (1H, m), 3.04 (6H, s), 3.73 (3H, s), 3.83–3.96 (2H, m), 4.97 (1H, t), 7.67 (1H, s). m/z $[\text{M} - \text{H}]^- = 226$. HPLC $t_R = 1.25$ min.

Methyl 2-Methylsulfanyl-4-[(2R)-tetrahydrofuran-2-yl]pyrimidine-5-carboxylate. 2-Methyl-2-thiopseudourea sulfate (1.54 g, 11.1 mmol) was added to methyl (Z)-3-(dimethylamino)-2-[(2R)-tetrahydrofuran-2-carbonyl]prop-2-enoate (1.8 g, 7.92 mmol) and sodium acetate (2.73 g, 33.3 mmol) in DMF (30 mL) at rt. The resulting solution was stirred at 80 °C for 3 h. Water was added to the cooled solution, the mixture was extracted with EtOAc, and the organic layer was washed with water, dried over MgSO₄, filtered, and evaporated. The resulting crude product was purified by FCC, elution gradient 5–30% EtOAc in isohexane, to afford the title compound (1.46 g, 73%) as a colorless oil. ¹H NMR (400 MHz, CDCl₃) 1.96–2.10 (3H, m), 2.38–2.49 (1H, m), 2.60 (3H, s), 3.91 (3H, s), 4.00–4.05 (1H, m), 4.13–4.19 (1H, m), 5.69–5.74 (1H, m), 8.88 (1H, s). *m/z* MH⁺ = 255. HPLC *t*_R = 1.88 min.

2-Methylsulfanyl-4-[(2R)-tetrahydrofuran-2-yl]pyrimidine-5-carboxylic acid. LiOH·H₂O (0.482 g, 11.48 mmol) in water (10 mL) was added to a stirred solution of methyl 2-methylsulfanyl-4-[(2R)-tetrahydrofuran-2-yl]pyrimidine-5-carboxylate (1.46 g, 5.74 mmol) in THF (20 mL) at rt. The resulting mixture was stirred at rt for 3 days and then partially evaporated. The resulting aqueous layer was washed with EtOAc and then was acidified with 1 M aqueous citric acid and extracted with EtOAc. The organic layer was washed with saturated brine, dried over MgSO₄, filtered, and evaporated to afford the title compound (1.23 g, 89%) as a white solid. ¹H NMR (400 MHz, CDCl₃) 1.99–2.20 (3H, m), 2.39–2.49 (1H, m), 2.62 (3H, s), 4.03–4.11 (1H, m), 4.16–4.22 (1H, m), 5.66–5.70 (1H, m), 9.02 (1H, s), CO₂H not observed. *m/z* MH⁺ = 241. HPLC *t*_R = 0.59 min.

***N*-(5-Hydroxy-2-adamantyl)-2-methylsulfanyl-4-[(2R)-oxolan-2-yl]pyrimidine-5-carboxamide.** *i*-Pr₂NEt (3.57 mL, 20.48 mmol) was added to 2-methylsulfanyl-4-[(2R)-tetrahydrofuran-2-yl]pyrimidine-5-carboxylic acid (1.23 g, 5.12 mmol), (1*S*,4*R*)-4-aminoadamantan-1-ol hydrochloride (1.043 g, 5.12 mmol), and 2-(3*H*-[1,2,3]triazolo[4,5-*b*]pyridin-3-yl)-1,1,3,3-tetramethylsauronium hexafluorophosphate(V) (HATU; 2.34 g, 6.14 mmol) in DMF (15 mL) at rt. The resulting solution was stirred at rt for 16 h and then was evaporated and taken up in EtOAc. The organic layer was washed with water and saturated brine, dried over MgSO₄, filtered, and evaporated, and the resulting crude product was purified by FCC, elution gradient 1–6% DCM in MeOH, to afford the title compound (1.18 g, 59%) as an off-white solid. ¹H NMR (400 MHz, CDCl₃) 1.50–1.59 (3H, m), 1.75–1.83 (6H, m), 1.90–1.97 (2H, m), 2.03–2.27 (6H, m), 2.59 (3H, s), 2.80–2.91 (1H, m), 3.89–3.93 (1H, m), 3.97–4.02 (1H, m), 4.20–4.26 (1H, m), 5.14 (1H, t), 7.91 (1H, d), 8.86 (1H, s). *m/z* MH⁺ = 390. HPLC *t*_R = 1.69 min.

***N*-(5-Hydroxy-2-adamantyl)-2-methylsulfonyl-4-[(2R)-oxolan-2-yl]pyrimidine-5-carboxamide.** 3-Chloroperoxybenzoic acid (70%) (1.392 g, 5.65 mmol) was added in one portion to *N*-(5-hydroxy-2-adamantyl)-2-methylsulfanyl-4-[(2R)-oxolan-2-yl]pyrimidine-5-carboxamide (1.1 g, 2.82 mmol) in DCM (45 mL) at 0 °C. The resulting solution was stirred at rt for 24 h. The reaction mixture was taken up in DCM and washed with saturated aqueous NaHCO₃ and saturated brine. The organic layer was dried over MgSO₄, filtered, and evaporated to afford the title compound (1.18 g, 99%) as a white solid. ¹H NMR (400 MHz, CDCl₃) 1.50–1.60 (3H, m), 1.74–1.85 (6H, m), 1.90–1.98 (2H, m), 2.08–2.31 (6H, m), 2.79–2.90 (1H, m), 3.36 (3H, s), 3.90–4.04 (2H, m), 4.23–4.30 (1H, m), 5.24 (1H, t), 7.88 (1H, d), 9.17 (1H, s). *m/z* MH⁺ = 422. HPLC *t*_R = 1.31 min.

2-[(2*S*,6*R*)-2,6-Dimethylmorpholin-4-yl]-*N*-(5-hydroxy-2-adamantyl)-4-[(2R)-oxolan-2-yl]pyrimidine-5-carboxamide (3). *N*-(5-Hydroxy-2-adamantyl)-2-methylsulfonyl-4-[(2R)-oxolan-2-yl]pyrimidine-5-carboxamide (12.3 g, 29.2 mmol) and (2*R*,6*S*)-2,6-dimethylmorpholine (15 mL, 121.1 mmol) were dissolved in THF (150 mL), and the resulting solution was stirred at rt for 24 h. The reaction mixture was evaporated and the crude product was purified by FCC, elution gradient 1–5% MeOH in EtOAc, and then triturated with diethyl ether to afford the title compound 3 (7.80 g, 59%) as a white solid. ¹H NMR (400 MHz, CDCl₃) 1.26 (6H, d), 1.41 (1H, s), 1.48–1.58 (2H, m), 1.75–1.85 (6H, m), 1.89–1.96 (2H, m), 2.01–2.09 (2H, m), 2.14–2.23 (4H, m), 2.62 (2H, t), 2.74–2.82 (1H, m), 3.57–3.66 (2H, m), 3.91 (1H, q), 3.98–4.03 (1H, m), 4.19–4.26 (1H,

m), 4.63 (2H, d), 5.08 (1H, t), 7.90 (1H, d), 8.75 (1H, s). *m/z* MH⁺ = 457. HPLC *t*_R = 1.96 min.

Ethyl 4-Hydroxy-2-methylthiazole-5-carboxylate (10). Thioacetamide (10.1 g, 134 mmol) was added to diethyl bromomalonate 9 (22.9 mL, 134 mmol) in toluene (77 mL). The reaction mixture was stirred at 110 °C for 90 min, allowed to cool to rt, filtered through Celite, and washed with toluene. The filtrate was evaporated and the residue was slurried in water for 5 min. The precipitate was collected by filtration and then washed with water and isohexane and dried in vacuo to afford the title compound 10 (6.18 g, 25%) as a pale yellow solid. ¹H NMR (400 MHz, DMSO) 1.22 (3H, t), 2.56 (3H, s), 4.17 (2H, q), 11.72 (1H, s). *m/z* MH⁺ = HATU188. HPLC *t*_R = 1.38 min.

Ethyl 4-Methoxy-2-methylthiazole-5-carboxylate. Diisopropyl azodicarboxylate (DIAD; 4.67 mL, 24.0 mmol) in THF (16.7 mL) was added to ethyl 4-hydroxy-2-methylthiazole-5-carboxylate 10 (3 g, 16.0 mmol), PPh₃ (4.62 g, 17.6 mmol), and MeOH (1.95 mL, 48.1 mmol) in THF (85 mL) at 10 °C. The reaction mixture was stirred at rt overnight and then heated at 50 °C for 2 h. The reaction mixture was concentrated in vacuo, and then 3:1 isohexane/EtOAc (50 mL) was added and the mixture was filtered. The filtrate was concentrated in vacuo and then partially purified by FCC, elution gradient 10–60% EtOAc in isohexane. The resulting impure product was dissolved in EtOAc and washed with 2 M aqueous NaOH, and the precipitate was discarded. The resulting organic layer was dried over MgSO₄, filtered, and evaporated to afford the title compound (1.56 g, 49%) as a colorless oil. ¹H NMR (400 MHz, DMSO) 1.22 (3H, t), 2.62 (3H, s), 4.01 (3H, d), 4.17 (2H, q). *m/z* MH⁺ = 202. HPLC *t*_R = 1.74 min.

4-Methoxy-2-methylthiazole-5-carboxylic Acid. Aqueous NaOH (2 M, 8.05 mL, 16.1 mmol) was added to ethyl 4-methoxy-2-methylthiazole-5-carboxylate (1.08 g, 5.37 mmol) in ethanol (20 mL), and the reaction mixture was stirred at rt for 1 h and then evaporated. The resulting residue was diluted with water and acidified with 2 M aqueous HCl (8.05 mL), and the resulting precipitate was isolated by filtration and dried in vacuo to afford the title compound (0.718 mg, 77%) as a white solid. ¹H NMR (400 MHz, DMSO) 2.67 (3H, s), 4.04 (3H, s), 12.64 (1H, s). *m/z* MH⁺ = 174. HPLC *t*_R = 1.01 min.

***N*-(trans-5-Hydroxy-2-adamantyl)-4-methoxy-2-methylthiazole-5-carboxamide (5).** HATU (1.14 g, 2.99 mmol) was added to a stirred solution of 4-methoxy-2-methylthiazole-5-carboxylic acid (431 mg, 2.49 mmol), (1*S*,4*R*)-4-aminoadamantan-1-ol hydrochloride (507 mg, 2.49 mmol), and *i*-Pr₂NEt (1.30 mL, 7.47 mmol) in DMF (5 mL), and the reaction mixture was stirred at rt for 17 h. The reaction mixture was poured onto water and extracted with EtOAc, and the combined organic layers were washed with saturated brine, dried over MgSO₄, filtered, and evaporated. The resulting crude product was purified by preparative HPLC to afford the title compound 5 (0.49 g, 61%) as a white solid. ¹H NMR (400 MHz, CDCl₃) 1.51–1.58 (1H, m), 1.69–1.83 (7H, m), 1.85–1.97 (2H, m), 2.12–2.22 (3H, m), 2.62 (3H, s), 4.16 (4H, d), 7.32 (1H, d), OH signal not observed. *m/z* MH⁺ = 323. HPLC *t*_R = 1.59 min.

Ethyl 2-Chloro-3-oxo-3-[(2R)-tetrahydrofuran-2-yl]propanoate. Sulfuryl chloride (12.0 mL, 149 mmol) was added dropwise to ethyl 3-oxo-3-[(2R)-tetrahydrofuran-2-yl]propanoate (27.7 g, 150 mmol) in DCM (500 mL) at 0 °C. The resulting solution was allowed to warm to rt and was stirred for 2 h and then quenched by pouring cautiously onto stirred water (250 mL). The organic layer was isolated, and the aqueous layer was extracted with DCM. The combined organic layers were washed with saturated brine, dried over MgSO₄, and evaporated to afford crude title compound (29.8 g, 91%) that was used without further purification. ¹H NMR (400 MHz, CDCl₃) 1.19–1.3 (3H, m), 1.78–1.93 (2H, m), 1.99–2.26 (2H, m), 3.76–3.9 (2H, m), 4.15–4.34 (2H, m), 4.45–4.59 (1H, m), 5.10 (1H, d). Mass ion not observed by LCMS.

Ethyl 2-Methyl-4-[(2R)-tetrahydrofuran-2-yl]thiazole-5-carboxylate. Ethanethioamide (232 mg, 3.08 mmol) was added to a stirred solution of crude ethyl 2-chloro-3-oxo-3-[(2R)-tetrahydrofuran-2-yl]propanoate (682 mg, 3.08 mmol if pure) in EtOH (6 mL), and the resulting solution was stirred at 80 °C for 90 min. The reaction mixture was allowed to cool to rt, evaporated, and purified by FCC, elution gradient 0–100% EtOAc in isohexane, to afford the title

compound (250 mg, 26%) as a yellow oil. ^1H NMR (400 MHz, DMSO) 1.26 (3H, t), 1.85–2.10 (3H, m), 2.13–2.26 (1H, m), 2.65 (3H, s), 3.78 (1H, td), 3.89–4.01 (1H, m), 4.26 (2H, q), 5.47–5.83 (1H, m). m/z MH^+ = 242. HPLC t_{R} = 1.84 min.

2-Methyl-4-[(2R)-tetrahydrofuran-2-yl]thiazole-5-carboxylic Acid. Aqueous NaOH (2 M, 1.55 mL, 3.11 mmol) was added to ethyl 2-methyl-4-[(2R)-tetrahydrofuran-2-yl]thiazole-5-carboxylate (250 mg, 1.04 mmol) in MeOH (4 mL). The reaction mixture was stirred at rt for 3 h and then acidified with 1 M aqueous citric acid and diluted with EtOAc, and the organic layer was isolated. The aqueous layer was extracted with EtOAc, and the combined organic layers were washed with water and saturated brine, dried over MgSO_4 , filtered, and evaporated to afford the title compound (215 mg, 97%) as a cream-colored solid. ^1H NMR (400 MHz, DMSO) 1.84–2.22 (4H, m), 2.64 (3H, s), 3.72–3.82 (1H, m), 3.89–3.98 (1H, m), 5.63 (1H, t), 13.39 (1H, br s). m/z MH^+ = 214. HPLC t_{R} = 0.66 min.

N-(trans-5-Hydroxy-2-adamantyl)-2-methyl-4-[(2R)-tetrahydrofuran-2-yl]thiazole-5-carboxamide (27). HATU (460 mg, 1.21 mmol) was added to a stirred solution of 2-methyl-4-[(2R)-tetrahydrofuran-2-yl]thiazole-5-carboxylic acid (215 mg, 1.01 mmol), (1S,4R)-4-aminoadamantan-1-ol hydrochloride (226 mg, 1.11 mmol), and *i*-Pr₂NEt (0.53 mL, 3.02 mmol) in DMF (5 mL), and the reaction mixture was stirred at rt for 17 h. The reaction mixture was poured onto water and extracted with EtOAc, and the combined organic layers were washed with saturated brine, dried over MgSO_4 , filtered, and evaporated. The resulting crude product was purified by preparative HPLC to afford the title compound 27 (150 mg, 41%) as a white solid. ^1H NMR (400 MHz, DMSO) 1.58 (2H, d), 1.72–2.04 (8H, m), 2.16 (5H, dd), 2.31–2.46 (1H, m), 2.51–2.71 (1H, m), 2.77 (3H, s), 3.97 (1H, td), 4.08 (2H, dd), 4.58 (1H, s), 5.26 (1H, t), 8.68 (1H, d). m/z MH^+ = 363. HPLC t_{R} = 1.70 min. HRMS (ES+) for C₁₉H₂₆N₂O₃S (MH⁺): calcd 363.1737, found 363.1735.

Ethyl 2-Amino-4-[(2R)-tetrahydrofuran-2-yl]thiazole-5-carboxylate. Thiourea (10.3 g, 135 mmol) was added to a solution of ethyl 2-chloro-3-oxo-3-[(2R)-tetrahydrofuran-2-yl]propanoate (29.8 g, 135 mmol) in ethanol (300 mL), and the resulting solution was stirred at 80 °C for 2 h. The reaction mixture was treated with triethylamine (18.9 mL, 135 mmol), evaporated, and purified by FCC, elution gradient 0.3–15% MeOH in DCM, to afford the title compound (26.5 g, 81%) as a pale yellow oil that crystallized upon standing. ^1H NMR (400 MHz, CDCl₃) 1.17–1.31 (3H, m), 1.75–2.05 (3H, m), 2.21–2.35 (1H, m), 3.78–3.87 (1H, m), 3.99–4.07 (1H, m), 4.1–4.26 (2H, m), 5.49 (1H, t), 5.87 (2H, s). m/z MH^+ = 243. HPLC t_{R} = 1.47 min.

Ethyl 2-Chloro-4-[(2R)-tetrahydrofuran-2-yl]thiazole-5-carboxylate. To a stirred suspension of ethyl 2-amino-4-[(2R)-tetrahydrofuran-2-yl]thiazole-5-carboxylate (26.5 g, 109 mmol) in 1,4-dioxane (100 mL) was added 4 M HCl in 1,4-dioxane (32.8 mL, 131 mmol) dropwise. The reaction mixture was stirred at rt for 30 min and evaporated. THF (300 mL) was added to the residue and the mixture was stirred at 65 °C before the dropwise addition of *tert*-butyl nitrite (17.1 mL, 142 mmol) as a solution in THF (50 mL) over 1 h. The reaction mixture was stirred for a further 1 h at 65 °C, cooled to rt, evaporated, and purified by FCC, eluting with 5–60% EtOAc in heptanes, to afford the title compound (22.4 g, 78%) as a pale yellow oil. ^1H NMR (400 MHz, DMSO) 1.28 (3H, t), 1.87–2 (2H, m), 2.01–2.12 (1H, m), 2.18–2.28 (1H, m), 3.77–3.84 (1H, m), 3.91–3.98 (1H, m), 4.26–4.33 (2H, m), 5.58–5.63 (1H, m). m/z MH^+ = 262. HPLC t_{R} = 2.26 min. A small amount of dechlorinated material ethyl 4-[(2R)-tetrahydrofuran-2-yl]thiazole-5-carboxylate (1.24 g, 5%) was obtained as a byproduct, and this was used to synthesize 29. ^1H NMR (400 MHz, DMSO) 1.29 (3H, t), 1.87–2.03 (2H, m), 2.05–2.15 (1H, m), 2.15–2.28 (1H, m), 3.76–3.84 (1H, m), 3.91–4.01 (1H, m), 4.24–4.35 (2H, m), 5.69 (1H, dd), 9.22 (1H, s). m/z MH^+ = 228. HPLC t_{R} = 1.62 min.

Methyl 2-Methoxy-4-[(2R)-tetrahydrofuran-2-yl]thiazole-5-carboxylate. A solution of 25% (w/w) NaOCH₃ in MeOH (2.23 g, 10.3 mmol) was added to a suspension of ethyl 2-chloro-4-[(2R)-tetrahydrofuran-2-yl]thiazole-5-carboxylate (2.70 g, 10.3 mmol) in MeOH (30 mL). The reaction mixture was heated in a microwave reactor at 100 °C for 6 h and then was allowed to cool to rt, diluted

with 1 M aqueous citric acid, and extracted with EtOAc. The organic layer was washed with water and saturated brine, dried over MgSO_4 , and evaporated. The resulting crude product was purified by FCC, elution gradient 20–100% EtOAc in heptanes, to afford the title compound (2.20 g, 85%) as a pale yellow foam. ^1H NMR (400 MHz, DMSO) 1.84–1.98 (2H, m), 2.03–2.20 (2H, m), 3.76–3.82 (1H, m), 3.79 (3H, s), 3.91–3.97 (1H, m), 4.06 (3H, s), 5.54–5.59 (1H, m). m/z MH^+ = 244. LCMS t_{R} = 1.88 min.

2-Methoxy-4-[(2R)-tetrahydrofuran-2-yl]thiazole-5-carboxylic acid. KOSi(CH₃)₃ (2.22 g, 17.3 mmol) was added to methyl 2-methoxy-4-[(2R)-tetrahydrofuran-2-yl]thiazole-5-carboxylate (2.10 g, 8.63 mmol) in THF (100 mL), and the reaction mixture was stirred at rt overnight. The reaction mixture was quenched with 1 M aqueous citric acid and extracted with EtOAc (100 mL). The organic layer was washed with water and saturated brine, dried over MgSO_4 , filtered, and evaporated to afford the title compound (1.90 g, 96%) as a yellow solid. ^1H NMR (400 MHz, DMSO) 1.84–1.98 (2H, m), 2.02–2.18 (2H, m), 3.71–3.78 (1H, m), 3.89–3.96 (1H, m), 4.03 (3H, s), 5.56–5.61 (1H, m), 13.25 (1H, br s). m/z MH^+ = 230. HPLC t_{R} = 1.39 min.

N-(trans-5-Hydroxy-2-adamantyl)-2-methoxy-4-[(2R)-tetrahydrofuran-2-yl]thiazole-5-carboxamide (36). HATU (3.78 g, 9.95 mmol) was added to a solution of 2-methoxy-4-[(2R)-tetrahydrofuran-2-yl]thiazole-5-carboxylic acid (1.90 g, 8.29 mmol), (1S,4R)-4-aminoadamantan-1-ol hydrochloride (2.53 g, 12.4 mmol), and *i*-Pr₂NEt (4.33 mL, 24.9 mmol) in DMF (25 mL). The reaction mixture was stirred at rt for 17 h and then was evaporated, diluted with water (50 mL), stirred for 10 min, and filtered. The resulting residue was washed with water, dried in vacuo, and then dissolved in EtOAc, dried over MgSO_4 , filtered, and evaporated. The resulting crude product was purified by crystallization from EtOAc to afford the title compound (1.70 g, 54%) as a cream-colored solid. ^1H NMR (400 MHz, DMSO) 1.38–1.47 (2H, m), 1.60–1.67 (4H, m), 1.69–1.80 (4H, m), 1.90–2.06 (5H, m), 2.16–2.27 (1H, m), 2.29–2.39 (1H, m), 3.80–3.85 (1H, m), 3.86–3.91 (1H, m), 3.90–3.98 (1H, m), 4.02 (3H, s), 4.41 (1H, s), 5.04 (1H, t), 8.50–8.57 (1H, m). m/z MH^+ = 379. HPLC t_{R} = 1.96 min. HRMS (ES+) for C₁₉H₂₆N₂O₄S (MH⁺): calcd 379.1686, found 379.1684.

2-Chloro-4-[(2R)-tetrahydrofuran-2-yl]thiazole-5-carboxylic acid. KOSi(CH₃)₃ (7.35 g, 57.3 mmol) was added to a solution of ethyl 2-chloro-4-[(2R)-tetrahydrofuran-2-yl]thiazole-5-carboxylate (5.00 g, 19.1 mmol) in THF (50 mL), and the reaction mixture was stirred at rt for 30 min. The reaction mixture was acidified with 4 M HCl in 1,4-dioxane (20 mL) and evaporated. The resulting residue was partitioned between DCM and 1 M aqueous citric acid. The organic layer was isolated and passed through a phase-separation cartridge and evaporated to afford the title compound (4.43 g, 99%) as a white solid. ^1H NMR (400 MHz, DMSO) 1.92–2.06 (2H, m), 2.14 (1H, ddd), 2.27 (1H, ddt), 3.82–3.9 (1H, m), 4.00 (1H, dd), 5.70 (1H, dd), 14.05 (1H, s). m/z MH^+ = 232, 234. HPLC t_{R} = 1.39 min.

2-Chloro-N-(5-hydroxy-2-adamantyl)-4-[(2R)-tetrahydrofuran-2-yl]thiazole-5-carboxamide. 1,1'-Carbonyldiimidazole (CDI; 4.02 g, 24.8 mmol) was added to 2-chloro-4-[(2R)-tetrahydrofuran-2-yl]thiazole-5-carboxylic acid (3.86 g, 16.5 mmol) in DMF (50 mL) at rt, and the resulting solution was stirred at rt for 90 min. (1S,4R)-4-Aminoadamantan-1-ol hydrochloride (3.37 g, 16.5 mmol) and 1,8-diazabicyclo[5.4.0]undec-7-ene (DBU; 4.94 mL, 33 mmol) were added, and the resulting solution was stirred at rt for 2 days. The reaction mixture was taken up in water and EtOAc and extracted with EtOAc. The combined organic layers were washed with brine, dried over MgSO_4 , evaporated, and purified by FCC, elution gradient 0–60% EtOAc in heptanes, to afford the title compound (4.16 g, 66%) as a yellow gum. ^1H NMR (400 MHz, DMSO) 1.43 (2H, d), 1.65 (4H, d), 1.69–1.83 (4H, m), 1.93–2.01 (2H, m), 2.05 (3H, d), 2.27 (2H, dt), 3.84 (1H, ddd), 3.94 (2H, dd), 4.43 (1H, s), 5.11–5.18 (1H, m), 8.72 (1H, d). m/z MH^+ = 383. HPLC t_{R} = 2.05 min.

N-(trans-5-Hydroxy-2-adamantyl)-4-[(2R)-tetrahydrofuran-2-yl]-2-tetrahydropyran-4-yloxythiazole-5-carboxamide (40). Sodium hydride (60% w/w in oil, 5.08 g, 127 mmol) was added to tetrahydro-2H-pyran-4-ol (81.0 mL, 846 mmol) in THF (40 mL) at 5 °C. The reaction mixture was stirred at 5 °C for 30 min, and then a

solution of 2-chloro-*N*-(5-hydroxy-2-adamantyl)-4-[(2*R*)-tetrahydrofuran-2-yl]thiazole-5-carboxamide (12.0 g, 28.2 mmol) in THF (40 mL) was added. The reaction was stirred at rt for 16 h and then was poured into 1 M aqueous citric acid and extracted with EtOAc. The combined organic layers were washed with brine, evaporated, purified by FCC, elution gradient 60–100% EtOAc in heptane, and then triturated with diethyl ether to afford the title compound (6.02 g, 48%) as a colorless solid. ¹H NMR (400 MHz, DMSO) 1.41 (2H, d), 1.63 (4H, d), 1.67–1.8 (6H, m), 1.93–2.09 (7H, m), 2.14–2.24 (1H, m), 2.26–2.36 (1H, m), 3.45–3.52 (2H, m), 3.78–3.85 (3H, m), 3.87–3.96 (2H, m), 4.42 (1H, s), 5.01–5.05 (2H, m), 8.51 (1H, d). *m/z* MH⁺ = 449. HPLC *t*_R = 1.99 min. HRMS (ES⁺) for C₂₃H₃₂N₂O₃S (MH⁺): calcd 449.2105, found 449.2100.

Ethyl 2-Chloro-3-cyclopropyl-3-oxopropanoate. Sulfuryl chloride (8.97 mL, 110 mmol) was added dropwise to a solution of ethyl 3-cyclopropyl-3-oxopropanoate (17.2 g, 110 mmol) in DCM (150 mL) at 0 °C. The reaction mixture was allowed to warm to rt and was stirred at rt for 90 min and then quenched by pouring slowly into water. The organic layer was isolated, the aqueous layer was extracted with DCM, and the combined organic layers were washed with water and saturated brine, dried over Na₂SO₄, and evaporated to afford impure ethyl 2-chloro-3-cyclopropyl-3-oxopropanoate (20.5 g, 98% if pure) that was used without purification or characterization.

Ethyl 2-Amino-4-cyclopropylthiazole-5-carboxylate. Thiourea (4.06 g, 53.4 mmol) was added to a stirred solution of crude ethyl 2-chloro-3-cyclopropyl-3-oxopropanoate (10.2 g, 53.4 mmol if pure) in EtOH (70 mL), and the resulting solution was stirred at 80 °C for 90 min. The resulting precipitate was isolated by filtration, washed with EtOH, and dried in vacuo to afford the title compound (9.93 g, 88%) as a white crystalline solid, which was used without further purification. ¹H NMR (400 MHz, DMSO) 0.89–0.98 (4H, m), 1.23 (3H, t), 2.80–2.88 (1H, m), 4.17 (2H, q), NH₂ not assigned. *m/z* MH⁺ = 213. HPLC *t*_R = 1.69 min.

Ethyl 2-Chloro-4-cyclopropylthiazole-5-carboxylate. HCl in 1,4-dioxane (4 M, 30 mL, 120 mmol) was added to a suspension of ethyl 2-amino-4-cyclopropylthiazole-5-carboxylate (9.70 g, 45.7 mmol) in 1,4-dioxane (50 mL), and the reaction mixture was stirred for 30 min and then evaporated. THF (150 mL) was added to the resulting white solid, and *tert*-butyl nitrite (8.22 mL, 68.6 mmol) was added dropwise at 65 °C over a period of 1 h. The reaction mixture was stirred at 65 °C for 1 h and then poured into water and extracted with EtOAc. The organic layer was isolated, dried over Na₂SO₄, evaporated, and purified by FCC, elution gradient 0–20% EtOAc in heptanes, to afford the title compound (7.40 g, 70%) as a colorless solid. ¹H NMR (400 MHz, DMSO) 1.00–1.07 (2H, m), 1.14–1.20 (2H, m), 1.35 (3H, t), 2.93–3.01 (1H, m), 4.36 (2H, q). *m/z* MH⁺ = 232. HPLC *t*_R = 2.92 min.

2-Chloro-4-cyclopropylthiazole-5-carboxylic Acid. KOSi(CH₃)₃ (8.31 g, 64.7 mmol) was added to a solution of ethyl 2-chloro-4-cyclopropylthiazole-5-carboxylate (5.00 g, 21.6 mmol) in THF (100 mL), and the reaction mixture was stirred at rt for 1 h. The reaction mixture was quenched with 4 M HCl in 1,4-dioxane and evaporated, and the resulting residue was taken up in DCM and water. The organic layer was isolated and evaporated to afford the title compound (4.39 g, 100%) as a pale yellow solid. ¹H NMR (400 MHz, DMSO) 0.91–0.97 (2H, m), 1.04–1.11 (2H, m), 2.94 (1H, m), CO₂H not observed. *m/z* MH⁺ = 204. HPLC *t*_R = 1.99 min.

2-Chloro-4-cyclopropyl-*N*-(5-hydroxy-2-adamantyl)thiazole-5-carboxamide. HATU (11.6 g, 30.6 mmol), (1*S*,4*R*)-4-amino-adamantan-1-ol hydrochloride (4.98 g, 24.5 mmol), and *i*-Pr₂NEt (10.6 mL, 61.1 mmol) were added to 2-chloro-4-cyclopropylthiazole-5-carboxylic acid (4.15 g, 20.4 mmol) in DCM (90 mL). The reaction mixture was stirred at rt for 2 h and then was taken up in DCM and water. The organic layer was isolated, dried over Na₂SO₄, evaporated, and purified by FCC, elution gradient 0–100% EtOAc in heptanes, to afford the title compound (6.56 g, 91%) as a solid. ¹H NMR (400 MHz, DMSO) 0.92–0.85 (m, 2H), 1.04–0.95 (m, 2H), 1.34 (d, 2H), 1.65–1.58 (m, 4H), 1.73–1.65 (m, 2H), 1.86 (d, 2H), 2.03–1.98 (m, 1H), 2.08 (s, 2H), 2.52–2.41 (m, 1H), 3.90–3.84 (m, 1H), 4.40 (s, 1H), 8.03 (d, 1H). *m/z* MH⁺ = 353. HPLC *t*_R = 2.04 min.

2-[(1-Cyanocyclopropyl)methoxy]-4-cyclopropyl-*N*-(trans-5-hydroxy-2-adamantyl)thiazole-5-carboxamide (51). Sodium hydride (60% w/w in oil, 0.51 g, 12.8 mmol) was added to 1-(hydroxymethyl)-cyclopropanecarbonitrile (1.24 g, 12.8 mmol) in THF (15 mL) at 0 °C. The reaction mixture was allowed to warm to rt and stirred for 30 min, and then 2-chloro-4-cyclopropyl-*N*-(5-hydroxy-2-adamantyl)-thiazole-5-carboxamide (1.5 g, 4.25 mmol) was added. The reaction mixture was stirred at rt for 16 h and then evaporated, and the residue was taken up in DCM and 1 M aqueous citric acid. The organic layer was isolated, evaporated, and purified by FCC, elution gradient 20–100% EtOAc in heptane, to afford the title compound **51** (1.41 g, 80%) as a white solid. ¹H NMR (400 MHz, DMSO) 0.86–0.97 (4H, m), 1.2–1.25 (2H, m), 1.31–1.39 (4H, m), 1.57–1.64 (4H, m), 1.65–1.72 (2H, m), 1.8–1.89 (2H, m), 1.95–2.01 (1H, m), 2.06–2.12 (2H, m), 2.43–2.52 (1H, m), 3.82–3.88 (1H, m), 4.38 (2H, s), 4.39 (1H, s), 7.57 (1H, d). *m/z* MH⁺ = 414. HPLC *t*_R = 1.98 min. HRMS (ES⁺) for C₂₂H₂₇N₃O₃S (MH⁺): calcd 414.1846, found 414.1842.

Human and Murine in Vitro 11β-HSD1 Inhibition: Homogeneous Time-Resolved Fluorescence Assay. The conversion of cortisone to the active steroid cortisol by 11β-HSD1 oxoreductase activity, can be measured by a competitive HTRF assay (CisBio International, R&D, Administration and Europe Office, In Vitro Technologies - HTRF/Bioassays BP 84175, 30204 Bagnols/Cèze Cedex, France; cortisol bulk HTRF kit, catalog no. 62CO2PEC). The evaluation of compounds described herein was carried out with a baculovirus-expressed N-terminal 6-His-tagged full-length human or murine 11β-HSD1 enzyme. The enzyme was purified from a detergent-solubilized cell lysate, on a copper chelate column. Compounds to be tested were dissolved in DMSO to 10 mM and diluted further in assay buffer containing 1% DMSO to 10-fold the final assay concentration. Diluted compounds were then plated into black 384-well plates (Matrix, Hudson, NH). The assay was carried out in a total volume of 20 μL consisting of cortisone (Sigma, Poole, Dorset, U.K., 160 nM), glucose 6-phosphate (Roche Diagnostics, 1 mM), NADPH (Sigma, Poole, Dorset, U.K., 100 μM), glucose-6-phosphate dehydrogenase (Roche Diagnostics, 12.5 μg/mL), ethylenediaminetetraacetic acid (EDTA; Sigma, Poole, Dorset, U.K., 1 mM), assay buffer (K₂HPO₄/KH₂PO₄, 100 mM) pH 7.5, recombinant human or murine 11β-HSD1 [at an appropriate dilution to give a viable assay window; an example of a suitable dilution may be 1:1000 dilution of stock enzyme] plus test compound. The assay plates were incubated for 25 min at 37 °C, after which time the reaction was stopped by the addition of 10 μL of 0.5 mM glyceric acid plus conjugated cortisol (D2). Anticortisol Cryptate (10 μL) was then added, and the plates were sealed and incubated for 6 h at rt. Fluorescence at 665 and 620 nm was measured and the 665/620 nm ratio was calculated by use of an Envision plate reader. These data were then used to calculate IC₅₀ values for each compound (Origin 7.5, Microcal software, Northampton, MA).

Human in Vitro 11β-HSD1 Inhibition: High-Performance Liquid Chromatography Assay. The assay was carried out in a total volume of 1 mL consisting of cortisone (Sigma, Poole, Dorset, U.K., 160 nM), ³H-cortisone (PerkinElmer, 20 nmol/L, 1 μCi/mL), glucose 6-phosphate (Roche Diagnostics, 1 mM), NADPH (Sigma, Poole, Dorset, U.K., 100 μM), glucose-6-phosphate dehydrogenase (Roche Diagnostics, 12.5 μg/mL), EDTA (Sigma, Poole, Dorset, U.K., 1 mM), assay buffer (K₂HPO₄/KH₂PO₄, 100 mM) pH 7.5, recombinant 11β-HSD1, diluted 10-fold over HTRF enzyme dilution (E/10), plus test compound. The assay plates were incubated for 5 h at 37 °C, after which time the reaction was stopped by the addition of 100 μL of 0.5 mM glyceric acid. Radiolabeled steroids were extracted with EtOAc, and samples were evaporated to dryness under nitrogen and resuspended in mobile phase for HPLC analysis (methanol/H₂O 50:50). Radiolabeled steroids were separated by reverse-phase HPLC (Agilent 1200) on a Kromasil C18 5 μm column, 4.6 mm × 250 mm (Crawford Scientific, Lanarkshire, U.K.) with methanol/H₂O (50:50) at a flow rate of 1.5 mL/min. Radioactivity was measured by use of a flow scintillation analyzer (Radiomatic series 500TR, Perkin-Elmer Analytical Instruments) with FLO-ONE software.

Procedures for Crystallization, Data Collection, and Structure Solution for 28 (4c7k) and 44 (4c7j) in Complex with Human 11 β -HSD1. Protein expression and purification was done as described previously.¹⁵ The protein was concentrated to 8 mg/mL in a buffer consisting of 20 mM *N*-(2-hydroxyethyl)piperazine-*N'*-ethanesulfonic acid (HEPES) pH 8.0, 100 mM NaCl, 2 mM TCEP, and 10 μ M NADP. Prior to crystallization compounds were added to the protein sample to yield a final compound concentration of 2 μ M. The final DMSO concentration was 1%. Crystals were grown by the hanging drop vapor diffusion method. Protein (0.5 μ L) was mixed with 0.5 μ L of well solution containing 20% PEG-3350 and 200 mM ammonium nitrate and allowed to equilibrate over a reservoir containing well solution. For data collection, crystals were briefly transferred to a well solution containing 20% glycerol and flash-frozen in liquid nitrogen. Diffraction data of 28 and 44 in complex with 11 β -HSD1 were collected at the European Synchrotron Radiation Facility (ESRF) or on a rotating-anode X-ray source to resolutions of 1.9 and 2.2 Å, respectively. Data were processed with MOSFLM³⁶ and scaled and further reduced by use of the CCP4 suite of programs.³⁷ Initial phasing was done by molecular replacement using 4bbs¹⁵ as a starting model. The initial models were further refined by alternative cycles of model rebuilding in Coot³⁸ and refinement in Refmac5³⁹ and/or AutoBuster.⁴⁰ In both data sets the $F_o - F_c$ difference maps showed positive density in the h-11 β -HSD1 active site, which allowed unambiguous modeling of the bound ligands in three out of the four molecules of the asymmetric unit, with mole bound inhibitors. Data collection and refinement statistics can be found in the Supporting Information (Table S1).

Han Wistar Rat Central Nervous System Penetration Model.

Male Han Wistar rats were sourced from the AstraZeneca breeding colony at Alderley Park, U.K. Compounds were dosed orally in a HPMC/Tween (0.5% Methocel/0.1% polysorbate) vehicle at 30 mg/kg ($n = 2$ rats/compound). Animals were euthanized at 1 h postdose, and terminal blood (100 μ L of blood +100 μ L of water) and brain samples were collected from each animal. Samples were frozen at -20 °C for storage prior to analysis. Blood samples (50 μ L) were protein-precipitated with ice-cold CH₃CN containing a generic internal standard [(*N*-(1-adamantyl)-2-(1,1-dioxothiolan-3-yl)sulfanylpiperidine-3-carboxamide)]. The samples were then mixed and centrifuged (4500g for 10 min). A portion (50 μ L) of the resulting supernatant was removed and diluted with water (300 μ L) for injection (50 μ L) onto the LC-MS/MS system. Brain samples were homogenized after addition of water (4 \times dilution by weight) by use of a FisherBrand 500 homogenizer (ThermoFisher Scientific, Loughborough, U.K.), and in a similar manner to above, a portion (50 μ L) of the resulting homogenate was then protein-precipitated with ice-cold CH₃CN containing internal standard, centrifuged, and diluted with water prior to injection onto the LC-MS/MS system. Blood and brain samples were quantified against freshly prepared calibration curves with standards at 1, 5, 10, 50, 100, 500, 1000, 2000, 5000, and 10 000 ng/mL, prepared in the same manner as above. Quality controls were run before and after the unknown samples at concentrations of 10, 100, and 1000 ng/mL. The LC-MS/MS system is as described, with a Surveyor MS Pump Plus HPLC pump (Thermo Fisher Scientific, Hemel Hempstead, U.K.) and a CTC Analytics HTS PAL autosampler (Presearch Ltd., Basingstoke, U.K.) used to introduce the samples to the mass spectrometer. Chromatography was performed on a Max-RP (50 mm \times 2.1 mm i.d., 5 μ M) HPLC column (Phenomenex, Macclesfield, U.K.) with mobile phase consisting of varying ratios of water containing 0.1% formic acid and methanol containing 0.1% formic acid, flow rate 750 μ L/min. Samples were analyzed on a TSQ Quantum Vantage mass spectrometer (ThermoFisher Scientific, Hemel Hempstead, U.K.). Parent and product masses were autotuned into the mass spectrometer via QuickQuan (version 2.4) and Xcalibur (version 2.1) software (ThermoFisher Scientific, San Jose, CA). The capillary temperature was 270 °C, the vaporizer temperature was 300 °C, and the sheath gas and auxiliary gas flows were set at 60 and 20 arbitrary units, respectively. Subsequent to analysis, the data were quantified by use of QuickCalc software (Gubb Inc., Alpharetta, GA) by back-calculation against the relevant calibration curve. A 1/ x

weighting was applied to the calibration curves, which were constructed via a quadratic fit. Relevant dilution factors were applied to the unknown samples (2-fold for blood samples, 4-fold for brain samples) and a brain/blood ratio was calculated for each animal; this ratio was used to benchmark the compounds. For the brain protein binding protocol, rat protein binding and drug-brain tissue binding were determined by equilibrium dialysis combined with liquid chromatography following protocols in the literature;^{41,42} thus the free brain/blood ratio could be determined.

Target Engagement in Rat. Determination of Corticosteroids in Tissue Samples. Rat corticosteroid concentrations were measured by published extraction methods.⁴³

Analysis of Plasma Samples for Drug Concentration. Rat blood (50 μ L) was protein-precipitated with 200 μ L of ice-cold MeCN containing internal standard. The samples were then centrifuged at 4500g for 10 min prior to dilution of a 50 μ L aliquot of the supernatant with 300 μ L of deionized water. The resulting extract (50 μ L) was injected onto the LC-MS/MS system for subsequent quantification. Unknown samples were measured against calibration standards prepared from control rat blood and subsequently spiked with analyte at known concentrations. Calibration standards were subjected to the same extraction procedure as the unknowns.

Analysis of Brain Tissue Samples for Drug Concentration. Whole rat brains were weighed and diluted 4 \times (w/v) with deionized water. The samples were then homogenized by use of a homogenization probe (Fisher Scientific, Loughborough, U.K.). The resulting homogenate (50 μ L) was protein-precipitated with 200 μ L of ice-cold MeCN containing an internal standard (a compound structurally similar to the analytes from the AstraZeneca compound library). The samples were then centrifuged at 4500g for 10 min prior to dilution of a 50 μ L aliquot of the supernatant with 300 μ L of deionized water. The resulting extract (50 μ L) was injected onto the LC-MS/MS system for subsequent quantification. Unknown samples were measured against calibration standards prepared from control brain and subsequently spiked with analyte at known concentrations. Calibration standards were subjected to the same extraction procedure as the unknowns.

LC-MS/MS Conditions. The chromatography system consisted of a HP1100 HPLC pump (Agilent, Cheshire, U.K.) and a HTS PAL autosampler (Presearch Ltd., Basingstoke, U.K.). The HPLC column used was a Synergy Max-RP 50 \times 2.1 mm (Phenomenex, Macclesfield, U.K.) maintained at a constant temperature of 50 °C. The mobile phase consisted of variable ratios of 0.1% formic acid in water and 0.1% formic acid in methanol, flow rate 0.75 mL/min. A TSQ Quantum Vantage MS fitted with a heated ES probe (ThermoFisher Scientific, Hemel Hempstead, U.K.). Compounds were auto-optimized for tube lens voltage, parent ion m/z , collision energy, and product ion m/z by use of QuickQuan version 2.1 software (ThermoFisher Scientific, San Jose, CA). The MS settings were generic for all compounds tested with spray voltage at 3500 V, vaporizer temperature at 350 °C, sheath and auxiliary gas pressure at 60 and 20 arbitrary units, respectively, capillary temperature at 270 °C, and collision cell pressure at 1.5 mTorr.

Treatment of Results. Corticosterone (Cort) and 11-dehydrocorticosterone (11-DHC) concentration levels were used to generate a Cort/11-DHC ratio for use in target engagement assessment. Compound levels in plasma and brain were combined with experimental protein binding values in the relevant tissues (see previous section) to generate free drug concentrations for the construction of Cort/11-DHC versus [free plasma] or [free brain] plots for the compound of interest.

Diet-Induced Obese Mouse Compound-in-Diet Experiment. Mice (C57B6, Alderley Park, U.K.) were housed in groups of three upon arrival and allowed ad-lib access to water and control or 60 kcal % fat rodent diet in meal form (D12492Mi Research Diet USA) for 30 weeks. Animals were acclimatized in scintainer and individually housed prior to study phase. Body weight was monitored weekly during high-fat feeding. At the start of study, animals were randomized on the basis of body weight ($n = 10$ each group). Animals were maintained on control or compound-containing diets for 25 days. Lean

controls were maintained on 10 kcal % fat control diet (D12450 Bi, Research Diets USA). Compounds were formulated 1 day prior to beginning of live phase. Compounds **51** (240 mg) and **40** (48, 144, or 480 mg) were weighed out into a marble mortar and crushed with pestle before addition to preweighed powdered diet (30 g). After mixing in a blender for 10 min, the compound/diet mixture was compressed into balls of approximately 28–30 g each and stored at 4 °C until use. Individual animals were fed 2.5 g of CID mix a day, and the chow mix was checked to ensure consumption. During the treatment phase, body weight and food intake were monitored 3 times a week at 8 a.m. (1 h before lights off). On day 21, following a 13 h fast, blood samples were taken by tail-prick for glucose measurements (Accu-Chek strip and read by Aviva Accu-Chek monitor). Each sampling was done within 2 min to minimize disturbance to the animals. Animals were re-fed following the procedures. Following a short recovery, on day 24 plasma exposure of individual animal was analyzed at 11 a.m. and 3 p.m.. Animals were terminated on day 25 at 9 a.m. without fast. Animals were euthanized by rising CO₂, and a blood sample was taken via cardiac bleed immediately. Plasma was frozen down for compound exposure, and liver samples were dissected for ex vivo enzyme activity measurement.

Ex Vivo Enzyme Activity. Liver samples were stored at –80 °C prior to assay. Liver samples were weighed (150–200 mg) and transferred to a 24-well plate on ice. Warmed medium [1 mL of Dulbecco's modified Eagle medium (DMEM) Ham F12 medium supplemented with 1% penicillin/streptomycin/ampicillin and 10% fetal calf serum (FCS)] containing 20 nM [³H]cortisone (1 μCi/mL, ~20 nM final assay concentration, NET1178001MC, lot no. 3632365, Perkin-Elmer) was added to the well, and tissue was cut into 2–3 mm³ pieces with scissors. Liver samples were incubated for 10 min at 37 °C in 95% O₂/5% CO₂. Following incubation, medium from liver assays was transferred to an Eppendorf tube and centrifuged (2 min, 3600 rpm), and the resulting supernatant was transferred to a 5-in. × 5/8-in. glass test tube prior to extraction. Extraction of radiolabeled steroids was carried out by the addition of 2.5 mL of EtOAc to each sample. Following a 10 s vortex mixing, the top solvent layer of each sample, containing the tritiated steroids, was transferred to a 4-in. × 4/8-in. glass tube. EtOAc was evaporated off at 50 °C, under nitrogen. Samples were resuspended in 140 μL of 1:1 MeOH/water (mobile phase). Samples were run on a HPLC-linked scintillation counter [Agilent 1200 system and Perkin-Elmer Flo-Scintillation analyzer (500TR)] with a Kromasil C18 5 μm column (4.6 mm × 250 mm). Each sample was run for 12 min at 50 °C with 1:1 MeOH/water at 1.5 mL/min.

Pharmacokinetics. On day 24 at 2 and 6 h from lights off, 20-μL blood samples were taken via conscious tail-prick and diluted immediately in 80 μL of phosphate-buffered saline (PBS) and centrifuged at 6000g for 10 min at 4 °C. Terminal blood sample was taken on day 25 at the time of lights off. Neat and diluted plasma samples were transferred to a 96-well plate and analyzed for compound exposure. HOMA-IR was defined from [fasting glucose (millimolar) × fasting insulin (milliunits per liter)]/22.5.

Pregnane X Receptor Inhibition Assay. A medium for cells was prepared: add supplements to DMEM-phenol red free (Mediatech) and warm at 37 °C in water bath [add 5 mL of nonessential amino acids (Mediatech) + 5 mL of 2 mM L-glutamine (Invitrogen) + 50 mL of 10% charcoal-stripped FBS (Hyclone)]. Test compounds were prepared from 10 mM stock solution DMSO by dilution to final concentrations of 10 and 1 μM. Initially compounds were diluted on plate to 4X the final assay concentration (40 μM) in HepG2 medium containing DMSO, and so 10 μL of stock was taken and diluted in 2490 μL of medium for a 250X dilution. The compound (1000 μL of 40 μM solution) was placed in a deep well place in one well, with 900 μL of blank medium in subsequent wells. Stock concentration of rifampicin (10 mM) and dexamethasone (30 mM) were made up. HepG2 cells, CryoTES (Applied Cell Sciences), were thawed by placing vials in a 37 °C water bath and HepG2 medium was added slowly to bring up to 40 mL volume, and then the samples were centrifuged and resuspended in 5 mL of HepG2 medium. Cell density and viability was determined by the trypan blue method and thus

adjusted to a concentration of 3.5 × 10⁵ cells/mL (350 000), and then cell suspension was added to each well (75 μL). Test compounds (25 μL) were transferred to give final concentrations of 10 and 1 μM, and the plate was incubated at 37 °C, 5% CO₂ for 72 h. After 72 h, a steadylite HTS assay kit was prepared (PerkinElmer 6016987, 500 mL kit) as per instructions to yield reconstituted substrate. The medium was aspirated off the plate and the cells were washed twice at rt with Dulbecco's PBS buffer (200 μL/well). Reconstituted substrate was added (100 μL/well) to the culture plate, and the plate was agitated gently under subdued light conditions. The plate was sealed and incubated for 5 min in the dark at rt and then transferred to a plate reader, and luminescence was measured. The result was expressed as a percentage of control at the two concentrations.

■ ASSOCIATED CONTENT

📄 Supporting Information

Additional text describing preparation and characterization for additional final compounds, and two tables listing data collection and refinement statistics for X-ray crystallography and parameters for PK/PD modeling. This material is available free of charge via the Internet at <http://pubs.acs.org>.

Accession Codes

The crystal structures of human 11β-HSD1 in complex with **28** and with **44** have been deposited in the Protein Data Bank (PDB accession codes 4c7k and 4c7j).

■ AUTHOR INFORMATION

Corresponding Authors

*Phone +44(0)1625519064; e-mail frederick.goldberg@astrazeneca.com.

*Phone +44(0)7720685539; e-mail al.dossetter@medchemica.com.

Notes

The authors declare no competing financial interest.

■ ACKNOWLEDGMENTS

We thank Brendan Leighton for his leadership of the bioscience strategy and for providing references, Peter Ceuppens for statistical support, Alice Yu for in vivo bioscience support, Elizabeth Kelly for running the DIO study, Pam Tyers for generating high-quality HPLC data, and Gisela Brändén and Cristian Bodin for their contributions to the X-ray crystallography work.

■ ABBREVIATIONS USED

CID, compound in diet; CDI, 1,1'-carbonyldiimidazole; DIAD, diisopropyl azodicarboxylate; DIO, diet-induced obese mice; FCC, flash column chromatography; HATU, 2-(3H-[1,2,3]-triazolo[4,5-b]pyridin-3-yl)-1,1,3,3-tetramethylisouronium hexafluorophosphate(V); hBA1c, glycated hemoglobin; HFD, 60% high fat diet of chow; HOMA-IR, homeostasis model assessment—insulin resistance; HPMC, hydroxypropyl methylcellulose; HRMS, high-resolution mass spectrometry; 11β-HSD1, 11β-hydroxysteroid dehydrogenase type 1; h-11β-HSD1, human isoform of 11β-hydroxysteroid dehydrogenase type 1; m-11β-HSD1, murine isoform of 11β-hydroxysteroid dehydrogenase type 1; HTRF, homogeneous time-resolved fluorescence; LLE, ligand lipophilicity efficiency; MDCK, Madin-Darby canine kidney; NADP(H), nicotinamide adenine dinucleotide phosphate (reduced); PEG, poly(ethylene glycol); POMC, proopiomelanocortin

REFERENCES

- (1) Edwards, C. R. W.; Benediktsson, R.; Lindsay, R. S.; Seckl, J. R. 11β -Hydroxysteroid dehydrogenases: key enzymes in determining tissue-specific glucocorticoid effects. *Steroids* **1996**, *61*, 263–269.
- (2) Walker, E. A.; Stewart, P. M. 11β -Hydroxysteroid dehydrogenase: unexpected connections. *Trends Endocrinol. Metab.* **2003**, *14*, 334–339.
- (3) Strain, G. W.; Zumoff, B.; Strain, J. J.; Levin, J.; Fukushima, D. K. Cortisol production in obesity. *Metab. Clin. Exp.* **1980**, *29*, 980–985.
- (4) Thieringer, R.; Hermanowski-Vosatka, A. Inhibition of 11β -HSD1 as a novel treatment for the metabolic syndrome: do glucocorticoids play a role? *Expert Rev. Cardiovasc. Ther.* **2005**, *3*, 911–924.
- (5) Walker, B. R. Glucocorticoids and cardiovascular disease. *Eur. J. Endocrinol.* **2007**, *157*, 545–559.
- (6) Tomlinson, J. W.; Walker, E. A.; Bujalska, I. J.; Draper, N.; Lavery, G. G.; Cooper, M. S.; Hewison, M.; Stewart, P. M. 11β -Hydroxysteroid dehydrogenase type 1: a tissue-specific regulator of glucocorticoid response. *Endocr. Rev.* **2004**, *25*, 831–866.
- (7) Yau, J. L.; Noble, J.; Kenyon, C. J.; Hibberd, C.; Kotelevtsev, Y.; Mullins, J. J.; Seckl, J. R. Lack of tissue glucocorticoid reactivation in 11β -hydroxysteroid dehydrogenase type 1 knockout mice ameliorates age-related learning impairments. *Proc. Natl. Acad. Sci. U.S.A.* **2001**, *98*, 4716–4721.
- (8) Holmes, M. C.; Carter, R. N.; Noble, J.; Chitnis, S.; Dutia, A.; Paterson, J. M.; Mullins, J. J.; Seckl, J. R.; Yau, J. L. 11β -Hydroxysteroid dehydrogenase type 1 expression is increased in the aged mouse hippocampus and parietal cortex and causes memory impairments. *J. Neurosci.* **2010**, *30*, 6916–6920.
- (9) Sandeep, T. C.; Yau, J. L.; MacLulich, A. M.; Noble, J.; Deary, I. J.; Walker, B. R.; Seckl, J. R. 11β -Hydroxysteroid dehydrogenase inhibition improves cognitive function in healthy elderly men and type 2 diabetics. *Proc. Natl. Acad. Sci. U.S.A.* **2004**, *101*, 6734–6739.
- (10) Scott, J. S.; Goldberg, F. W.; Turnbull, A. V. Medicinal chemistry of 11β -hydroxysteroid dehydrogenase type 1 (11β -HSD1). *J. Med. Chem.* [Online early access]. DOI: 10.1021/jm4014746. Published online: December 2, 2013.
- (11) Anagnostis, P.; Katsiki, N.; Adamidou, F.; Athyros, V. G.; Karagiannis, A.; Kita, M.; Mikhailidis, D. P. 11β -Hydroxysteroid dehydrogenase type 1 inhibitors: novel agents for the treatment of metabolic syndrome and obesity-related disorders? *Metabolism* **2013**, *52*, 21–33.
- (12) Rosenstock, J.; Banarer, S.; Fonseca, V. A.; Inzucchi, S. E.; Sun, W.; Yao, W.; Hollis, G.; Flores, R.; Levy, R.; Williams, W. V.; Seckl, J. R.; Huber, R. The 11β -hydroxysteroid dehydrogenase type 1 inhibitor INCB13739 improves hyperglycemia in patients with type 2 diabetes inadequately controlled by metformin monotherapy. *Diabetes Care* **2010**, *33*, 1516–1522.
- (13) Bauman, D. R.; Whitehead, A.; Contino, L. C.; Cui, J.; Garcia-Calvo, M.; Gu, X.; Kevin, N.; Ma, X.; Pai, L.-Y.; Shah, K.; Shen, X.; Stribling, S.; Zokian, H. J.; Metzger, J.; Shevell, D. E.; Waddell, S. T. Evaluation of selective inhibitors of 11β -HSD1 for the treatment of hypertension. *Bioorg. Med. Chem. Lett.* **2013**, *23*, 3650–3653.
- (14) Shah, S.; Hermanowski-Vosatka, A.; Gibson, K.; Ruck, R. A.; Jia, G.; Zhang, J.; Hwang, P. M. T.; Ryan, N. W.; Langdon, R. B.; Feig, P. U. Efficacy and safety of the selective 11β -HSD1 inhibitors MK-0736 and MK-0916 in overweight and obese patients with hypertension. *J. Am. Soc. Hypertens.* **2011**, *5*, 166–176.
- (15) Goldberg, F. W.; Leach, A. G.; Scott, J. S.; Snelson, W. L.; Groombridge, S. D.; Donald, C. S.; Bennett, S. N. L.; Bodin, C.; Gutierrez, P. M.; Gyte, A. C. Free-Wilson and structural approaches to co-optimizing human and rodent isoform potency for 11β -hydroxysteroid dehydrogenase type 1 (11β -HSD1) inhibitors. *J. Med. Chem.* **2012**, *55*, 10652–10661.
- (16) Bisschop, P. H.; Dekker, M. J.; Osterthun, W.; Kwakkel, J.; Anink, J. J.; Boelen, A.; Unmehopa, U. A.; Koper, J. W.; Lamberts, S. W.; Stewart, P. M.; Swaab, D. F.; Fliers, E. Expression of 11β -hydroxysteroid dehydrogenase type 1 in the human hypothalamus. *J. Neuroendocrinol.* **2013**, *25*, 425–32.
- (17) Savontaus, E.; Conwell, I. M.; Wardlaw, S. L. Effects of adrenalectomy on AGRP, POMC, NPY and CART gene expression in the basal hypothalamus of fed and fasted rats. *Brain Res.* **2002**, *958*, 130–138.
- (18) Beaulieu, S.; Gagné, B.; Barden, N. Glucocorticoid regulation of proopiomelanocortin messenger ribonucleic acid content of rat hypothalamus. *Mol. Endocrinol.* **1988**, *2*, 727–731.
- (19) Scott, J. S.; Bowker, S. S.; deSchoolmeester, J.; Gerhardt, S.; Hargreaves, D.; Kilgour, E.; Lloyd, A.; Mayers, R. M.; McCoull, W.; Newcombe, N. J.; Ogg, D.; Packer, M. J.; Rees, A.; Revill, J.; Schofield, P.; Selmi, N.; Swales, J. G.; Whittamore, P. R. O. Discovery of a potent, selective, and orally bioavailable acidic 11β -hydroxysteroid dehydrogenase type 1 (11β -HSD1) inhibitor: Discovery of 2-[(3S)-1-[5-(cyclohexylcarbonyl)-6-propylsulfanylpyridin-2-yl]-3-piperidyl]-acetic acid (AZD4017). *J. Med. Chem.* **2012**, *55*, 5951–5964.
- (20) Scott, J. S.; deSchoolmeester, J.; Kilgour, E.; Mayers, R. M.; Packer, M. P.; Hargreaves, D.; Gerhardt, S.; Ogg, D. J.; Rees, A.; Selmi, N.; Stocker, A.; Swales, J. G.; Whittamore, P. R. O. Novel acidic 11β -hydroxysteroid dehydrogenase type 1 (11β -HSD1) inhibitor with reduced acyl glucuronide liability: The discovery of 4-[4-(2-adamantylcarbonyl)-5-tert-butyl-pyrazol-1-yl]benzoic acid (AZD8329). *J. Med. Chem.* **2012**, *55*, 10136–10147.
- (21) Scott, J. S.; Gill, A. L.; Godfrey, L.; Groombridge, S. D.; Rees, A.; Revill, J.; Schofield, P.; Sörme, P.; Stocker, A.; Swales, J. G.; Whittamore, P. R. O. Optimisation of pharmacokinetic properties in a neutral series of 11β -HSD1 inhibitors. *Bioorg. Med. Chem. Lett.* **2012**, *22*, 6756–6761.
- (22) Di, L.; Rong, H.; Feng, B. Demystifying brain penetration in central nervous system drug discovery. *J. Med. Chem.* **2013**, *56*, 2–12.
- (23) The absolute configuration of **3** was established from synthesis from (2R)-tetrahydrofuran-2-carboxylic acid. The corresponding S analogue was much less potent against both the human (IC_{50} 1.2 μ M) and mouse (IC_{50} 2.1 μ M) forms of 11β -HSD1.
- (24) Desai, P. V.; Raub, T. J.; Blanco, M.-J. How hydrogen bonds impact P-glycoprotein transport and permeability. *Bioorg. Med. Chem. Lett.* **2012**, *22*, 6540–6548.
- (25) Heffron, T. P.; Salphati, L.; Alicke, B.; Cheong, J.; Dotson, J.; Edgar, K.; Goldsmith, R.; Gould, S. E.; Lee, L. B.; Lesnick, J. D.; Lewis, C.; Ndubaku, C.; Nonomiya, J.; Olivero, A. G.; Pang, J.; Plise, E. G.; Sideris, S.; Trapp, S.; Wallin, J.; Wang, L.; Zhang, X. The design and identification of brain penetrant inhibitors of phosphoinositide 3-kinase α . *J. Med. Chem.* **2012**, *55*, 8007–8020.
- (26) Bissantz, C.; Kuhn, B.; Stahl, M. A medicinal chemist's guide to molecular interactions. *J. Med. Chem.* **2010**, *53*, 5061–5084.
- (27) Kotelevtsev, Y.; Brown, R. W.; Fleming, S.; Kenyon, C.; Edwards, C. R. W.; Seckl, J. R.; Mullins, J. J. Hypertension in mice lacking 11β -hydroxysteroid dehydrogenase type 2. *J. Clin. Invest.* **1999**, *103*, 683–689.
- (28) Wan, Z.; Chenail, E.; Xiang, J.; Li, H.; Ipek, M.; Bard, J.; Svenson, K.; Mansour, T. S.; Xu, X.; Tian, X.; Suri, V.; Hahm, S.; Xin, Y.; Johnson, C. E.; Li, X.; Qadri, A.; Panza, D.; Perreault, M.; Tobin, J. F.; Saiah, E. Efficacious 11β -hydroxysteroid dehydrogenase type I inhibitors in the diet-induced obesity mouse model. *J. Med. Chem.* **2009**, *52*, 5449–5461.
- (29) Harno, E.; Cottrell, E. C.; Yu, A.; deSchoolmeester, J.; Gutierrez, P. M.; Denn, M.; Swales, J. G.; Goldberg, F. W.; Bohlooly-Y, M.; Andersén, H.; Wild, M. J.; Turnbull, A. V.; Leighton, B.; White, A. 11β -HSD1 inhibitors still improve metabolic phenotype in male 11β -HSD1 knock-out mice suggesting off-target mechanisms. *Endocrinology* **2013**, *154* (10), 4580–4593.
- (30) Fotsch, C.; Bartberger, M. D.; Bercot, E. A.; Chen, M.; Cupples, R.; Emery, M.; Fretland, J.; Guram, A.; Hale, C.; Han, N.; Hickman, D.; Hungate, R. W.; Hayashi, M.; Komorowski, R.; Liu, Q.; Matsumoto, G.; St. Jean, D. J., Jr.; Ursu, S.; Veniant, M.; Xu, G.; Ye, Q.; Yuan, C.; Zhang, J.; Zhang, X.; Tu, H.; Wang, M. Further studies with the 2-amino-1,3-thiazol-4(SH)-one class of 11β -hydroxysteroid dehydrogenase type 1 inhibitors: reducing pregnane X receptor activity and exploring activity in a monkey pharmacodynamic model. *J. Med. Chem.* **2008**, *51*, 7953–7967.

(31) Zhu, Y.; Olson, S. H.; Hermanowski-Vosatka, A.; Mundt, S.; Shah, K.; Springer, M.; Thieringer, R.; Wright, S.; Xiao, J.; Zokian, H.; Balkovec, J. M. 4-Methyl-5-phenyl triazoles as selective inhibitors of 11 β -hydroxysteroid dehydrogenase type I. *Bioorg. Med. Chem. Lett.* **2008**, *18*, 3405–3411.

(32) Gao, Y. D.; Olson, S. H.; Balkovec, J. M.; Zhu, Y.; Royo, I.; Yabut, J.; Evers, R.; Tan, E. Y.; Tang, W.; Hartley, D. P.; Mosley, R. T. Attenuating pregnane X receptor (PXR) activation: A molecular modelling approach. *Xenobiotica* **2007**, *37*, 124–138.

(33) Marino, J. P., Jr.; Mcatee, J. J.; Washburn, D. G. Preparation of nitrogen heterocyclic compounds, particularly substituted piperidines and pyrrolidines, as soluble epoxide hydrolase (sEH) and 11 β -hydroxysteroid dehydrogenase type 1 (11 β -HSD1) inhibitors and their use. World Patent WO2009070497, 2009.

(34) Iyer, A.; Kauter, K.; Alam, M. A.; Hwang, S. H.; Morisseau, C.; Hammock, B. D.; Brown, L. Pharmacological inhibition of soluble epoxide hydrolase ameliorates diet-induced metabolic syndrome in rats. *Exp. Diabetes Res.* **2012**, 758614.

(35) Luria, A.; Bettaieb, A.; Xi, Y.; Shieh, G. J.; Liu, H. C.; Inoue, H.; Tsai, H. J.; Imig, J. D.; Haj, F. G.; Hammock, B. D. Soluble epoxide hydrolase deficiency alters pancreatic islet size and improves glucose homeostasis in a model of insulin resistance. *Proc. Natl. Acad. Sci. U.S.A.* **2011**, *108*, 9038–9043.

(36) Leslie, A. G. Integration of macromolecular diffraction data. *Acta Crystallogr.* **2006**, *D62*, 48–57.

(37) Collaborative Computational Project 4. The CCP4 suite: Programs for protein crystallography. *Acta Crystallogr.* **1994**, *D50*, 750–763.

(38) Emsley, P.; Cowtan, K. Coot: model-building tools for molecular graphics. *Acta Crystallogr.* **2004**, *D60*, 2126–2132.

(39) Murshudov, G. N.; Vagin, A. A.; Lebedev, A.; Wilson, K. S.; Dodson, E. J. Efficient anisotropic refinement of macromolecular structures using FFT. *Acta Crystallogr.* **1999**, *D55*, 247–255.

(40) Blanc, E.; Roversi, P.; Vonrhein, C.; Flensburg, C.; Lea, S. M.; Bricogne, G. Refinement of severely incomplete structures with maximum likelihood in BUSTER-TNT. *Acta Crystallogr.* **2004**, *D60*, 2210–2221.

(41) Wan, H.; Rehgren, M. High-throughput screening of protein binding by equilibrium dialysis combined with liquid chromatography and mass spectrometry. *J. Chromatogr. A* **2006**, *1102*, 125–134.

(42) Wan, H.; Rehgren, M.; Giordanetto, F.; Bergstrom, F.; Tunek, A. High-throughput screening of drug-brain tissue binding and in silico prediction for assessment of central nervous system drug delivery. *J. Med. Chem.* **2007**, *50*, 4606–4615.

(43) Rönquist-Nii, Y.; Edlund, P. O. Determination of corticosteroids in tissue samples by liquid chromatography–tandem mass spectrometry. *J. Pharm. Biomed. Anal.* **2005**, *37*, 341–350.